



## Effect of fineness and citric acid addition on the hydration of ye'elimité

Yassine El Khessaimi, Youssef El Hafiane, Agnès Smith

### ► To cite this version:

Yassine El Khessaimi, Youssef El Hafiane, Agnès Smith. Effect of fineness and citric acid addition on the hydration of ye'elimité. Construction and Building Materials, 2020, 258, pp.119686. 10.1016/j.conbuildmat.2020.119686 . hal-02935778

HAL Id: hal-02935778

<https://unilim.hal.science/hal-02935778>

Submitted on 22 Aug 2022

**HAL** is a multi-disciplinary open access archive for the deposit and dissemination of scientific research documents, whether they are published or not. The documents may come from teaching and research institutions in France or abroad, or from public or private research centers.

L'archive ouverte pluridisciplinaire **HAL**, est destinée au dépôt et à la diffusion de documents scientifiques de niveau recherche, publiés ou non, émanant des établissements d'enseignement et de recherche français ou étrangers, des laboratoires publics ou privés.



Distributed under a Creative Commons Attribution - NonCommercial 4.0 International License

1       Effect of fineness and citric acid addition on the hydration of ye'elimité

2       Y. EL KHESSAIMI<sup>1,2</sup>, Y. EL HAFIANE<sup>1</sup>, A. SMITH<sup>1</sup>

3       <sup>1</sup> IRCER, UMR CNRS 7315, Université de Limoges, Centre Européen de la Céramique, 12 avenue Atlantis,  
4       87068 Limoges cedex.

5       <sup>2</sup> Materials Science and Nano-engineering Department. Mohammed VI Polytechnic University. Lot 660.Hay  
6       Moulay Rachid.43150 Ben Guerir. Morocco.

7       Abstract

8       The first purpose of this article is to investigate the effect of fineness on the hydration of highly pure  
9       ye'elimité powders prepared by solid state reaction or by a chemical route. The second purpose is to  
10      examine the role of fineness on the hydration of model calcium sulfoaluminate cements (CSA)  
11      prepared by mixing our lab-made ye'elimité with gypsum. The last part concerns the effect of citric  
12      acid addition on hydration of a model cement. The main results are the following: (i) ettringite and  
13      hydrates formation can be accelerated by the presence of very fine ye'elimité powder in a CSA  
14      cement paste; (ii) the hydration rate of CSA model cement depends mainly on the dissolution rate of  
15      ye'elimité which can be delayed by the addition of citric acid in water; (iii) the surface of ye'elimité  
16      grains presents scarce etch pits when citric acid is present in the water, while the surface seems to be  
17      totally attacked with water.

18       Keywords

19       Ye'elimité; Fineness; Citric acid; Ettringite; Monosulfoaluminate; Gibbsite; Hydration; CSA cement.

20       Highlights

- 21       ■ Hydration of very fine ye'elimité powder prepared by sol-gel method;  
22       ■ The influence of ye'elimité fine microstructure on its hydration was studied for the first  
23      time;  
24       ■ The formation of etch-pits during ye'elimité dissolution;

- 25       ■ Ye'elmite dissolution governs the hydration rate of CSA model cement;
- 26       ■ Citric acid delays the dissolution of ye'elmite grains;
- 27       ■ Ettringite formation can be accelerated by the addition of highly fine ye'elmite powder;
- 28       ■ Ettringite formation can be delayed by the addition of citric acid.

29       1. Introduction

30       For their shrinkage compensation and self-stressing properties, Calcium Sulfoaluminate Cements  
31       (CSA) have been developed and produced in China since the last forty years [1]. More recently, the  
32       interest of the international cement research community towards these cements comes not only from  
33       their expansive behaviour [2], but also from their environmentally friendly characteristics associated  
34       to their production, which includes a reduced CO<sub>2</sub> footprint. However, many barriers prevent more  
35       widespread usage of this material. Despite having been used in construction for many years [3]  
36       relatively little is known about effective mixture design methodology for using CSA cement in  
37       concrete infrastructure. In the absence of formalized design guidance, CSA cements are most  
38       commonly used in small-scale repairs, where their ability to set rapidly can be advantageous and  
39       long working times are not necessary. For larger scale placements, retardation of the CSA reactions  
40       is necessary, and citric acid is currently the primary set retarding carboxylic acid recommended for  
41       use with CSA cements. However, the mechanism by which citric acid solutions modify the hydration  
42       of CSA cements is still not fully understood. Effect of citric acid addition on CSA cement hydration  
43       has been well recognized, and studied by several researchers, most of the studies were either based  
44       on qualitative description of hydration curves or parameters that indirectly refer to hydration, such as  
45       set time and strength [4–7]. Organic compounds like sugars or citric, tartaric or gluconic acids and  
46       their salts are powerful retarders in CSA cements [7]. Citrate and tartrate ions are chelating agents of  
47       Ca<sup>2+</sup> and Al<sup>3+</sup> and would be expected to influence the nucleation and growth of phases containing  
48       these ions [8]. Most carboxylic acids have no effect on the morphology of ettringite crystals. This  
49       probably results from the fact that the calcium ions of the crystals are buried in a sheet of negatively  
50       charged hydroxyl and water molecules and the negatively charged carboxylate groups are repelled by

51 the negatively charged crystals [8]. The mechanism through which citric acid influences the  
52 hydration kinetics of the CSA systems is not fully understood. However, researchers have found that  
53 citrate will form chelates with calcium on the surface of a cement, thus hindering cement dissolution,  
54 in addition to forming chelates with calcium ions already in solution and reducing their availability  
55 for participation in hydration reactions [9]. Another inorganic retarder acid applied for CSA-type  
56 cements is boric acid, it inhibits the nucleation of ettringite, but instead it allows six-sided plates of  
57 the metastable monosulfoaluminate phase to form [8,10].

58 The first authors who worked on the influence of citric acid on hydration reactions in the  
59  $3\text{CaO} \cdot \text{Al}_2\text{O}_3 \cdot \text{CaSO}_4 \cdot 2\text{H}_2\text{O} \cdot \text{CaO} \cdot \text{H}_2\text{O}$  system were Tinnea and Young [5]. They found that hydration  
60 reactions are retarded by the addition of citric acid. Ettringite and monosulfoaluminate were all  
61 detected as early hydration products. The influence of citric acid as a retarder for ternary binders  
62 based on Ordinary Portland Cements (OPC), CSA and anhydrite was investigated by Winnefeld et  
63 al. [6]. Their main conclusions were that the addition of citric acid retarded the early ettringite  
64 formation, lengthened the workability time, and reduced significantly the compressive strength even  
65 after 28 days. Zhang et al. [11] studied the effect of citric acid on the fluidity and strength of CSA  
66 commercial cements. They found that the initial fluidity of paste admixed with superplasticizers  
67 would be decreased by the presence of citric acid. Moreover, both early and late strengths of cement  
68 were decreased by the addition of citric acid. In a recent study about the effect of citric acid on  
69 hydration properties of commercial CSA, Burris et al. [4] found that citric acid successfully retarded  
70 initial set by 120 min for CSA cement. Despite the reported studies about the effect of citric acid on  
71 CSA cements hydration, there is a lack of understanding about how changing retarder dosage  
72 influences cement hydrates formation. It represents a serious barrier to specification and, in  
73 particular, larger scale usage of CSA cements.

74 From a materials scientist point of view, one parameter which dictates the reactivity of a powder  
75 (with water for instance, or during sintering) is its fineness. Cement fineness is considered as one of  
76 the major variables influencing cement properties and concrete strength [12–15]. It is also a  
77 dominant factor that affects cement hydration since the fineness directly controls the volume of

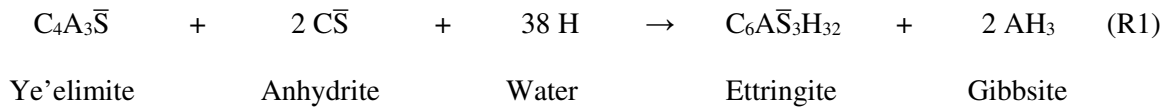
78 water available for hydration for each unit volume of cement particle, as well as the inter-particle  
79 spacing between them [16]. The aim of nanoparticle addition in cements is the stimulation of  
80 nucleation processes during the early cement hydration. The earlier these nuclei are formed, the  
81 earlier they can grow to larger crystals of hydration phases and thereby accelerate the cement  
82 hydration [17].

83 In the literature on cementitious materials and specifically Portland cements, different authors  
84 mentioned the effect of fineness on hydration [12,18–22]. Thomas [19] examined the hydration of  
85 the  $\beta$  polymorph of belite (calcium di-silicate). He observed that if this polymorph had a specific  
86 surface area similar to a Portland cement, it was less reactive with water than a  $\beta$ -belite prepared by a  
87 chemical route (Pechini process). Pollman [20] and Hong [21] indicated that the interest in using  
88 chemical synthesis methods was to be able to study the hydration behaviour of pure belite and in  
89 particular fine particles. The interplay between fineness and chemical composition of fillers  
90 (limestone, alumina, silica) on Portland mortars hydration was studied by Kadri et al. [13]. Whatever  
91 the type of filler, the finer it is, the more accelerated the early hydration of the mortar is. Fineness  
92 can also influence Portland concrete properties such as self-compaction, shrinkage, durability or  
93 reduction of product cost. A study is needed to accurately interpret the hydration process and  
94 quantify effects of cement fineness on CSA cement hydration and the role of ye'elimité fineness on  
95 hydration has not been studied.

96 Cement hydration is a complex process, because cement powder contains several inorganic phases.  
97 A simple way to well investigate the effect, is to examine the hydration of the main reactive  
98 cementitious phase in different controlled hydration conditions. CSA cements can have highly  
99 variable compositions, but all of them contain the key-phase ye'elimité,  $\text{Ca}_4(\text{AlO}_2)_6\text{SO}_4$  (noted  
100  $\text{C}_4\text{A}_3\bar{\text{S}}$  in cementitious notation) [23–25].

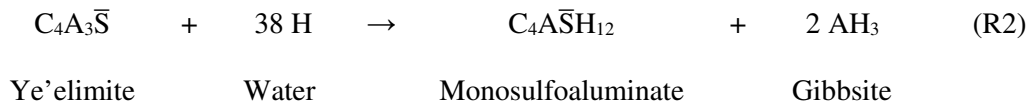
101 In fact, ye'elimité hydration proceeds through dissolution and precipitation [26], leading to the  
102 precipitation of various hydrates. In the presence of anhydrite (calcium sulfate,  $\text{CaSO}_4$  or  $\text{C}\bar{\text{S}}$ ),

103 ye'elimites hydrates to form ettringite  $\text{Ca}_6\text{Al}_2(\text{SO}_4)_3(\text{OH})_{12} \cdot 26\text{H}_2\text{O}$  or  $(\text{C}_6\text{A}\bar{\text{S}}_3\text{H}_{32})^*$  as well as gibbsite  
104  $\text{Al}(\text{OH})_3$  or  $(\text{AH}_3)$  (Reaction 1) [2,27–29]:



105

106 In the absence of calcium sulfate, the hydration of ye'elimites can lead to the formation of  
107 monosulfoaluminate ( $\text{Ca}_4\text{Al}_2(\text{SO}_4)(\text{OH})_{12} \cdot 6\text{H}_2\text{O}$  or  $\text{C}_4\text{A}\bar{\text{S}}\text{H}_{12}$ ) and gibbsite (Reaction 2) [2,27–29]:



108 Recently, significant work has been carried out on ye'elimites single phase hydration, pioneered by  
109 Hanic et al. [30]. Ye'elimites hydration was shown to occur through a two-step reaction. The reaction  
110 product in the first step was ettringite, whereas monosulfoaluminate  $\text{C}_4\text{A}\bar{\text{S}}\text{H}_{12}$  was the hydration  
111 product in the second step of hydration reaction. Suspensions of synthetic ye'elimites in a saturated  
112 gypsum solution were also investigated [31]. The most voluminous hydration product observed was  
113 ettringite. During the hydration of orthorhombic ye'elimites in dilute suspensions with a water over  
114 binder mass ratio equal to 40 and 100, Bullerjahn et al. [32] identified five stages of hydration: stage  
115 I (initial period), stage II (dormant period), stage III (acceleration period), stage IV (main hydration  
116 period) and stage V (final period). The duration of each stage was directly linked to the evolution of  
117 the solution concentrations and the type of hydration reaction [33]. Other authors were interested in  
118 the hydration behavior of orthorhombic and pseudo-cubic ye'elimites [34–36]. It was shown that in  
119 the absence of additional sulfate sources, orthorhombic-ye'elimites reacts slower than pseudo-cubic-  
120 ye'elimites, and monosulfoaluminate phases are the main hydrated crystalline phases (see reaction  
121 R2). However, in the presence of additional sulfates, orthorhombic-ye'elimites reacts faster than  
122 pseudo-cubic-ye'elimites, and the main hydrated crystalline phase is ettringite (see reaction R1). The  
123 published data on ye'elimites single phase hydration [34–37] are summarized in Fig. 1, which shows

---

\*The cement phase notations are used in this work ( $\text{C} = \text{CaO}$ ,  $\text{A} = \text{Al}_2\text{O}_3$ ,  $\bar{\text{S}} = \text{SO}_3$ ,  $\bar{\text{C}} = \text{CO}_2$ ,  $\text{H} = \text{H}_2\text{O}$ )

124 the degree of ye'elimitate hydration ( $\alpha$ ) (Fig. 1a) and the amount of the formed hydrates (Figs 1b, 1c  
125 and 1d). The degree of ye'elimitate hydration,  $\alpha$ , is calculated as follows:

$$\alpha(\%) = \frac{\text{wt}\%^{\text{ye'elimitate}}(t_0) - \text{wt}\%^{\text{ye'elimitate}}(t)}{\text{wt}\%^{\text{ye'elimitate}}(t_0)} \times 100 \quad (\text{E.1})$$

126 where ( $\text{wt}\%^{\text{ye'elimitate}}$ ) refers to the weight percentage of ye'elimitate, ( $t_0$ ) is the starting hydration time  
127 and ( $t$ ) is the final hydration time, the hydration duration corresponds to ( $t-t_0$ ). The amounts of  
128 formed hydrates (see Figs. 1b to 1d), namely ettringite, monosulfoaluminate and gibbsite, are  
129 directly extracted from the literature data. The plots show that depending on the authors, a large  
130 range of hydration degrees,  $\alpha$ , can be found in the literature. Besides, ye'elimitate hydration degree  
131 influences upon the amount of the formed hydrates, especially ettringite, and it depends on  
132 parameters, such as the presence of minor elements (iron, sodium) and the initial water over cement  
133 mass ratio. Thereby, physical and chemical characteristics of ye'elimitate play a significant role on  
134 CSA hydrates formation. The study of ye'elimitate hydration under controlled conditions of fineness  
135 and citric acid dosages can contribute to better understand the link between these two parameters and  
136 CSA cement hydration.

137

138 In this context, this paper tends to clarify the effect of these two factors, namely fineness and citric  
139 acid addition, on the hydration of ye'elimitate-rich cements. It can contribute to a better understanding  
140 of the early age expansion of industrial expansive CSA [38]. The paper starts by discussing the effect  
141 of fineness and citric acid addition on the dissolution of pure ye'elimitate powder prepared by solid  
142 state reaction or by a chemical route; for the first part of the work, the pure ye'elimitate powder is in  
143 dilute suspensions. Then, in a second part of the work, model CSA cements are prepared by mixing  
144 pure ye'elimitate with gypsum. In order to prepare cement pastes, these model cements are mixed with  
145 water alone or water containing citric acid. The aim is to examine how citric acid can influence the  
146 hydration kinetics and the chemical nature of the hydrated products. The studied CSA model systems  
147 show a schematic picture of the early behaviour of commercial CSA cements [38]. Despite the fact

148 that model cements do not reflect the whole complexity of commercial products, it helps to give a  
149 basic understanding of the hydration by focussing on the major hydration reactions [38].  
150 The experimental approach of the present study focuses on identifying the nature and the amount of  
151 the hydration products using Rietveld analysis coupled to TGA analysis and on monitoring the  
152 ye'elimité dissolution using continuous ionic conductivity measurement. Zeta potential  
153 measurements were also carried out to examine the mechanisms by which citric acid acts on  
154 ye'elimité-rich cement hydration.

155 **2. Materials and methods**

156 **2.1. Materials**

157 Ye'elimité  $\text{C}_4\text{A}_3\bar{\text{S}}$  powder was synthesized by solid state reactions from a 4:3:1 stoichiometric  
158 mixture of calcium carbonate ( $\text{CaCO}_3$ , CAS number: 471-34-1, Sigma-Aldrich, >99.9 wt.%),  
159 alumina ( $\text{Al}_2\text{O}_3$ , CAS number: 1344-28-1, Acros-Organics, >99.7 wt.%) and highly pure gypsum  
160 ( $\text{CaSO}_4 \cdot 2\text{H}_2\text{O}$ , CAS number: 10101-41-4, Sigma-Aldrich, >99.0 wt.%) powder. The raw materials  
161 were dry homogenized. The homogenized powders were then pressed into pellets (20 mm in  
162 diameter) and heated at 1300°C for 3 h. After 3 h, the samples were quenched in air. The pellets  
163 were reground with an excess of anhydrite in order to compensate sulfate volatilization during  
164 thermal treatment and then the powder was pressed again into disks before further heating. The  
165 pellets were quenched in air after this last heating and finally ground with an agate mortar. A  
166 detailed description about the synthesis protocol can be found in [25]. The sample was labelled: **Ye-**  
167 **sol.**

168 Ye'elimité was also synthesised by sol-gel method using the Organic Steric Entrapment route (OSE).  
169 A stoichiometric mixture of three salts ( $\text{Ca}(\text{NO}_3)_2 \cdot 4\text{H}_2\text{O}$ , CAS number: 13477-34-4, Fisher  
170 Scientific, >99.0 wt.%), ( $\text{Al}(\text{NO}_3)_2 \cdot 9\text{H}_2\text{O}$ , CAS number: 7784-27-2, Fisher Scientific, >99.0 wt.%),  
171 and ( $\text{Al}_2(\text{SO}_4)_3 \cdot 16\text{H}_2\text{O}$ , CAS number: 17927-65-0, Fisher Scientific, >98.0 wt.%) was added to a 5  
172 wt.% aqueous solution of (PVA, CAS number: 9002-89-5, VWR Chemicals). The resulting gel was

173 dried, then finely ground and finally calcined at 1250°C for 1 h. More details about the synthesis  
174 protocol can be found in [39]. The sample was labelled: **Ye-chem**.

175 Since ye'elite hydration depends on  $C_4A_3\bar{S}$  polymorphs [34,35], only orthorhombic ye'elite  
176 powders were synthesised to minimize parameters affecting hydration. In this respect, Ye-sol and  
177 Ye-chem refer to orthorhombic ye'elite phase. The synthesised ye'elite powders were found  
178 highly pure, with the presence of some impurities such as CA and CA<sub>2</sub>. In other works, C<sub>3</sub>A and  
179 C<sub>12</sub>A<sub>7</sub> were detected as impurities [25,39–41]. The presence of calcium aluminate impurities depends  
180 on the kinetic of solid state reactions during ye'elite formation. It was shown that the kinetic  
181 depends mainly on alumina grain size used as a raw material for ye'elite lab-synthesis [42].

182 To prepare a CSA model cement, Ye-sol was blended with gypsum CaSO<sub>4</sub>.2H<sub>2</sub>O (C $\bar{S}$ H<sub>2</sub> in  
183 cementitious notation) (CAS number: 10101-41-4, Sigma-Aldrich, > 99.0 wt.%). In order to examine  
184 the effect of citric acid on ye'elite hydration, commercial citric acid (HOC(CH<sub>2</sub>CO<sub>2</sub>H)<sub>2</sub>CO<sub>2</sub>H,  
185 CAS number: 77-92-9, Sigma-Aldrich) was used.

186 The different samples and the corresponding characterization techniques are summarized in [Table 1](#).

187 [2.2. Characterisation methods](#)

188 [2.2.1. XRD-Quantitative Rietveld analysis](#)

189 X-Ray Diffraction (XRD) data were collected at room temperature in the Bragg-Brentano geometry  
190 using a Bruker D8 Advance X-ray diffractometer with CuK $\alpha$  radiation ( $\lambda_{Cu} = 1.54056 \text{ \AA}$ , without  
191 monochromator; operating voltage of 40 kV and electric current 40 mA). The step scan was 0.02°  
192 with a time counting per step of 0.45 seconds. The sample was rotated during data collection at 15  
193 rpm in order to increase particle statistics. The diffractometer was equipped with an energy-  
194 dispersive LYNXEYE XE-T detector for filtration of fluorescence and K $\beta$  radiation. Mineral phases  
195 of the synthesised samples were quantified by using the Rietveld method as implemented in the  
196 TOPAS 4.2 software. The fitting parameters were the background coefficients, the phase scales, the  
197 zero-shift error, the cell parameters, and the phase shape parameters. The peak shapes were fitted  
198 using the pseudo-Voigt function. The Rietveld refinement strategy and the criteria for selecting the

best crystal structure data were based on the recent methods concerning diffraction and crystallography applied to anhydrous cements published by De la Torre et al. [43]. The structures used for fitting the crystalline phases and the respective ICSD (Inorganic Crystal Structure Database) codes [44–48] are given in [Table 2](#). To check the Rietveld fitting quality between measured and calculated diffractograms, reliability factors should be given as,  $R_{wp}$  (weighted profile R-factor),  $R_{exp}$  (expected R-factor) and GOF (Goodness Of Fit) [49]. These reliability factors reflect the deviation between measured intensities ( $I_{iM}$ ) and calculated intensities ( $I_{iC}$ ) at any given measurement point (i) as follows:

$$R_{wp} = \sqrt{\frac{\sum_i w_i (I_{iM} - I_{iC})^2}{\sum_i w_i (I_{iM})^2}} \quad (E.2)$$

$$R_{exp} = \sqrt{\frac{N-P}{\sum_i w_i (I_{iM})^2}} \quad (E.3)$$

$$GOF = \left( \frac{R_{wp}}{R_{exp}} \right)^2 \quad (E.4)$$

where  $w_i$  is the attributed weight, N is the number of data points and P is the number of the refined parameters.

Most of  $AH_3$  gel produced during CSA hydration (see reaction R1) is an amorphous phase [50]. In the present paper only crystalline gibbsite was quantified by XRD-Rietveld analysis. Since cement pastes and set cements contain a complex mix of different crystalline and amorphous hydrates, an accurate quantification by Rietveld analysis is sometimes difficult [51,52]. Therefore, our data are considered to be semi-quantitative and absolutely not quantitative.

## 2.2.2. Scanning Electron Microscopy (SEM)

The prepared samples were examined with a LEO 1530 VP field emission scanning electron microscopy (SEM) equipped with an Energy Dispersive X-ray Spectroscopy (EDS) detector (Oxford INCA 250). The microscope was operated at a 1 kV accelerating voltage. This low voltage is necessary in order to avoid spoiling the sample. The samples were stored in desiccators filled with

silica gel prior to and after examination in order to prevent hydration or carbonation. SEM observations were carried out without using a deposited conducting layer. For ye'elimitate dissolution experiments, ye'elimitate powder was stirred with demineralized water at 500 rpm using a magnetic agitator for the desired time. Hydration was stopped by the solvent exchange method using acetone, then filtered by vacuum aspiration and the samples could then be observed under the SEM.

#### 2.2.2. Particle size distribution (PSD) and BET specific surface area (SSA)

The PSD was measured in ethanol suspension using Horiba Partica LA-950-V2® applying the Fraunhofer model. Refractive indices of 1.568 and 1.525 were used for ye'elimitate  $C_4A_3S^-$  and gypsum  $CSH_2$ , respectively [31]. The SSA was estimated from  $N_2$  adsorption/desorption isotherm experiments using a Micromeritics model Asap® 2020 analyzer. Prior to measurements, a degassing step of the sample powder was carried out under vacuum at 110°C during 24 h.

#### 2.2.3. Thermogravimetry (TGA)

TGA was carried out in  $N_2$  atmosphere on 30 mg of sample using a SETARAM Labsys TG-DTA/DSC thermal analyser at 10 °C/min up to 1100°C.

#### 2.2.4. Continuous ionic conductivity measurement (IC)

The ionic conductivity measurements with time of ye'elimitate suspensions were performed using a CDM210 Conductivity Meter. The water over ye'elimitate weight ratio, W/C, is equal to 1000 (Fig. 2). This high dilution has been chosen to avoid the formation of hydrates and in order to have specifically information about ye'elimitate dissolution. During the measurement, the suspension was stirred at 500 rpm. The volume of the measurement cell is about 150 ml. The temperature was controlled by a thermostatic bath with external water circulation at 25 °C. Similar experiments were carried out with gypsum alone.

#### 2.2.5. Zeta potential measurement (ZP)

The interaction between the added citric acid and ye'elimitate powder was evaluated by measuring the zeta potential of ye'elimitate particles as a function of the citric acid concentration. Suspensions of 0.1 wt.% were prepared by mixing for 24 h ye'elimitate powder with deionized water containing different

245 dosages of citric acid (0 wt.%, 5 wt.% and 10 wt.% relative to the weight of ye'elimit powder). The  
246 zeta potential was measured using a Malvern ZetaSizer Nano ZS, which is based on the  
247 electrophoresis method.

248 Zeta potential values depend on pH value of the measured suspension. In the present experiments,  
249 when 0 wt.%, 5 wt.% and 10 wt.% of citric acid were added, the pH values of the corresponding  
250 suspensions were 11.79, 10.84 and 10.80. Therefore, pH values do not vary greatly with the addition  
251 of citric acid and the measured Zeta potential values are considered to be taken at pH from 10.8 to  
252 11.79.

### 253 [2.3. Experimental protocols](#)

254 [Fig. 2](#) and [Fig. 3](#) summarize the experimental protocols relevant to the preparation and the  
255 characterisation of the prepared suspensions and cement pastes.

#### 256 [2.3.1. Preparation of suspensions for ye'elimit dissolution experiments \(Fig. 2\)](#)

257 To gain information on the effect of ye'elimit grain fineness on the dissolution kinetics, two  
258 suspensions were compared; the first one contained ye'elimit powder synthesised by solid state  
259 reactions (**Ye-sol**), and the second one contained ye'elimit powder synthesised by sol-gel method  
260 (**Ye-chem**). All suspensions were made by adding the ye'elimit powder to the demineralized water  
261 with a water over ye'elimit weight ratio, W/C, equal to 1000. The suspension was stirred at 500  
262 rpm. To examine the influence of citric acid on ye'elimit dissolution, three different concentrations  
263 of citric acid were first dissolved in the demineralized water prior to mixing with the powder. The  
264 quantities of citric acid were equal to 0 wt.%, 5 wt.% and 10 wt.% relative to the weight of  
265 ye'elimit powder; they are labelled **Ye-Sol-0**, **Ye-Sol-5** and **Ye-Sol-10**, respectively. The chosen  
266 citric acid dosages are much higher than the common concentration ranges generally used to delay  
267 CSA hydration [4,7,11,53,54]. These dosages were chosen in order to allow us to highlight clearly  
268 the effect of citric acid addition on hydration.

#### 269 [2.3.2. CSA model cements pastes preparation \(Fig. 3\)](#)

270 CSA model cements were prepared by dry mixing gypsum with ye'elimitite powder either synthesised  
271 by solid state reaction (labelled: **CSA-sol**) or synthesised by sol-gel method (labelled: **CSA-chem**).  
272 The cement powders were prepared with a ye'elimitite to gypsum weight ratio, (Ye/Gy) of 2. The  
273 hydration was studied on cement pastes with a water to cement (cement = Ye + Gy) weight ratio,  
274 W/C of 2. Performing the hydration study at these chosen Ye/Gy and W/C ratios should allow full  
275 ettringite precipitation [27]. The pastes were mixed, sealed in polyethylene containers and stored at  
276 20°C for 3 days, 7 days and 28 days. These durations correspond to typical storage conditions for  
277 testing various properties of set cements (EN 196-1 [55]).

278 To study the influence of citric acid on the hydration of CSA model cement, three different  
279 concentrations of citric acid were pre-dissolved in the mixing water, equivalent to 0 wt.%, 0.5 wt.%  
280 and 1 wt.% relative to ye'elimitite powder weight, labelled **CSA-sol-0**, **CSA-sol-0.5** and **CSA-sol-1**,  
281 respectively. The chosen citric acid dosages are within the common concentration ranges generally  
282 used to retard CSA cements [4,7,11,53,54]. After completion of the expected hydration durations, the  
283 hydration process was stopped, and samples were kept in a dry atmosphere (desiccator filled with  
284 silica gel) until analysis.

285 [2.3.3. Hydration stoppage method](#)

286 The solvent exchange method was used to stop the hydration of the hydrated pastes. To this end, the  
287 hydrated paste was smoothly ground in an agate mortar and then mixed in 150 ml of acetone for 6  
288 min. Afterwards, the liquid was filtered from the sample by vacuum filtration.

289 [3. Results and discussion](#)

290 [3.1. PSD and BET of ye'elimitite and gypsum](#)

291 In our previous works concerning ye'elimitite synthesis [25,39], the mineralogical composition  
292 determined by XRD-quantitative Rietveld analysis, particle size distribution (PSD), powder  
293 microstructure and BET specific surface area (SSA) of the two-synthesised ye'elimitite powders were  
294 studied ([Table 3](#)). The micrographs and the BET data show that Ye-chem powder presents a smaller  
295 average grain size (136 nm) and a higher specific surface area (2.2 m<sup>2</sup>/g), in comparison to Ye-sol

296 powder, which has (2  $\mu\text{m}$ ) and ( $0.74 \text{ m}^2/\text{g}$ ) as average grain size and specific surface area,  
297 respectively. On the contrary, the particle size distribution measured by laser diffraction reveals  
298 higher  $D_{50}$  for Ye-chem powder (27.1  $\mu\text{m}$ ) than for Ye-sol (14.6  $\mu\text{m}$ ). This is due to the  
299 agglomeration state of Ye-chem powder as shown in SEM micrographs in [Table 3](#).

300 In order to prepare the CSA model cements, highly pure gypsum (> 99.0 wt.%) was used. It has the  
301 following characteristics:  $4.19 \text{ m}^2/\text{g}$  as BET surface area, and particle size diameters equal to  $d_{10} =$   
302 9.92  $\mu\text{m}$ ,  $d_{50} = 23.08 \mu\text{m}$  and  $d_{90} = 45.32 \mu\text{m}$ .

303 [3.2. Effect of fineness and citric acid on ye'elimitate dissolution](#)

304 The dissolution rate of anhydrous cementitious phases is proportional to the slope of the ionic  
305 conductivity versus time curves during the first minutes of dissolution. [Fig. 4a](#) shows the ionic  
306 conductivity variations of the Ye-sol-0, Ye-sol-5, Ye-sol-10 and Ye-chem suspensions (W/C=1000).  
307 Provided the temperature remains constant, the ionic conductivity in these highly dilute situations  
308 depends mainly on two factors: concentration of ions and ionic mobility. In the present situation, as  
309 soon as the powder is in contact with water, dissolution of ye'elimitate grains starts and the ions go  
310 into solution. Since the concentration of ions starts increasing, the ionic conductivity also increases  
311 immediately. It reaches a plateau with Ye-chem after 25 min. The slope value (s) of the different  
312 ionic conductivity curves ([Fig. 4a](#)) during the first minutes of dissolution ( $\sim 5 \text{ min}$ ) are in the  
313 following order:  $s(\text{Ye-chem-0}) > s(\text{Ye-sol-0}) > s(\text{Ye-sol-5}) > s(\text{Ye-sol-10})$ . In this later case, it  
314 looks as if there is no dissolution within 50 min since the ionic conductivity level remains constant.  
315 Thus, the corresponding dissolution rates (r) follow the following sequence as well:  $r(\text{Ye-chem-0}) >$   
316  $r(\text{Ye-sol-0}) > r(\text{Ye-sol-5}) > r(\text{Ye-sol-10}) \approx 0$ . Referring to similar conductivity measurements on  
317 gypsum suspensions with different citric acid content, respectively 0 wt.% (Gy-0), 5 wt.% (Gy-5)  
318 and 10 wt.% (Gy-10) ([Fig. 4b](#)), it seems that citric acid does not delay gypsum dissolution kinetics.  
319 The slope value of the different ionic conductivity curves ([Fig. 4b](#)) during the first minutes of  
320 dissolution ( $\sim 5 \text{ min}$ ) are almost equal. This means that citric acid does not delay gypsum dissolution  
321 kinetic and only influences upon ye'elimitate dissolution.

To investigate the morphological aspect of ye'elimit grains at early age dissolution stage, SEM micrographs of Ye-chem (Ye-chem-0) and that of Ye-sol powder immersed during 1 min in deionised water (Ye-sol-0), or in 10 wt.% citric acid solution (Ye-sol-10) are shown in Fig. 5. The water to ye'elimit ratio was 1000. After only 1 min, ye'elimit grains immersed in deionised water (Ye-sol-0, Fig. 5a, and Ye-chem-0, Fig. 5c) show a severely corroded surface with the formation of several etch-pits (holes on the micrographs). In the case of ye'elimit which has been in contact with a citric acid solution (Ye-sol-10, Fig. 5b), the ye'elimit grains surface appears smooth and much less attacked; moreover, the scarce etch-pits present characteristic geometries of crystal dissolution [56]. The SEM observations are in agreement with the (IC) measurements and confirm that the chemical nature of the solution in contact with ye'elimit plays an important role on its dissolution. The formation of etch-pits during mineral dissolution has been evidenced in the literature for other cementitious anhydrous phases such as alite (tricalcium silicate, C<sub>3</sub>S) and belite (dicalcium silicate, C<sub>2</sub>S) [56–59] and other silicates like quartz [60–62]. In fact, the formation of such etch-pits was previously observed on the surface of alite phase grains, the major phase in ordinary Portland cements, by Juillard et al. [56], who stated that etch-pits formation depends on the over/under saturation state of solution, and also on the crystallographic defects density of anhydrous alite grains. Nicoleau et al. [58] confirmed the discussions of Juillard et al. [56] concerning etch-pits formation during alite dissolution, by measuring the dissolution rate of alite according to the solution saturation state. The notion of etch-pits formation during mineral dissolution was identified and theorised early by Lasaga et al. [63] and Burch et al. [64] who observed etch-pits formation during dissolution experiments of quartz and calcium carbonates.

The rapid reactivity of ye'elimit powder synthesised by sol-gel method (Ye-chem) during the early dissolution step could be explained by its microstructure. In fact, Ye-chem powder shows very small ye'elimit grains ( $136 \pm 48$  nm, Table 3) compared to Ye-sol powder which contains relatively larger ye'elimit grains ( $2 \pm 1.2$   $\mu\text{m}$ , Table 3). This morphological difference provides ye'elimit surfaces with different reactivity to water.

349 To highlight the interaction between the added citric acid and ye'elimitite powder, zeta potential  
350 measurements were carried out on the ye'elimitite suspensions, Ye-sol-0, Ye-sol-5 and Ye-sol-10. The  
351 pH values of the corresponding acidic suspensions were 11.79, 10.84 and 10.80, respectively. Citric  
352 acid is normally considered to be a tri acid, with pKa values at 25 °C, extrapolated to zero ionic  
353 strength, of 2.92, 4.28, and 5.21 [65]. Thereby, citrate is the dominant form of citric acid present in  
354 our suspensions. The results of zeta potential measurements are shown in [Table 4](#). An increase in the  
355 citric acid concentration from 0 to 5 wt. % leads to a shift of the zeta potential from  $7.7 \pm 0.3$  mV to -  
356  $0.2 \pm 0.1$  mV, and the zeta potential turns to lower negative values ( $-10.9 \pm 2.8$  mV) for Ye-sol-10.  
357 The adsorption of citrate molecules at the surface of ye'elimitite grains could explain this change of  
358 zeta potential values. In citrate, the distances between two oxygen atoms in two neighbouring  
359 carboxylate groups, are between 2.7 and 4.0 Å ([Fig. 6a](#)) [66]. For ye'elimitite, the  $(13\bar{1})$  plane is a  
360 possible face for a ye'elimitite crystal [67]; the distances between two calcium atoms are between 3.0  
361 and 4.0 Å ([Fig. 6b](#)). Therefore, the citrate molecules can adsorb on the  $(13\bar{1})$  faces via the oxygen of  
362 the carboxylate groups to form a chelate. The remaining carboxylate functions of the adsorbed citrate  
363 molecules are negatively charged and can be responsible for the negative values of the zeta potential.  
364 This citrate adsorption can inhibit ye'elimitite grains dissolution. In solution, calcium and citrate can  
365 form chelates too [68]. Consequently, two events can explain the slow setting of cement paste  
366 containing ye'elimitite: the adsorption of citrate at the surface of ye'elimitite grains can delay  
367 ye'elimitite dissolution, and the formation of chelates between calcium and citrate in the solution can  
368 prevents calcium ions to participate in hydrates formation. The concept of citrate adsorption on  
369 gypsum crystals was adopted by different authors [68–70] to the explain the retarding effect on  
370 plaster crystallisation.

371 Another possible way to explain the effect of citric acid addition in the shifting of the zeta potential  
372 from positive values to negative values, is to use Bomblet's approach [71]. This author estimated the  
373 surface charge of alite ( $C_3S$ ) particles, and he showed that there are three times fewer positive sites  
374 than negative sites. Similarly, Smith et al. [72] applied Bomblet's approach to estimate the surface  
375 charge of krotite particles (calcium aluminate, CA) and they found that the negative sites are

376 dominant. The approach is based on a statistical representation of the charges on the surface of  
377 grains. It can be expressed as follows:

$$\frac{\sigma^+}{\sigma^-} \text{ is proportional to } \frac{\sum_{\text{positive ions}} r_+^2}{\sum_{\text{negative ions}} r_-^2} \quad (\text{E.5})$$

378 where  $\frac{\sigma^+}{\sigma^-}$  is the positive to negative surface charge ratio,  $r_+$  is the ionic radius associated to positive  
379 ions and  $r_-$  is the ionic radius associated to negative ions.

380 The application of this approach to ye'elimit starts by knowing the ionic radius of each element:

381 1.35 Å for oxygen, 1.05 Å for calcium, 0.5 Å for aluminium and 0.43 Å for sulphur.  $\frac{\sigma^+}{\sigma^-}$  can be  
382 calculated and it is proportional to 0.2. This means that the negative sites are dominant and that the  
383 surface of the anhydrous  $\text{C}_4\text{A}_3\bar{\text{S}}$  ( $\text{Ca}_4\text{Al}_6\text{O}_{16}\text{S}$ ) particles is consequently negatively charged.  
384 Assuming that all of the calcium ions of the surface form chelates molecules when citrate is present,

385 the  $\frac{\sigma^+}{\sigma^-}$  ratio becomes equal to 0.05. This means that negative sites become more dominant. Since zeta  
386 potential of a cement suspension is proportional to the surface charge of the cement grains present in  
387 this solution [72], the shift of ( $\zeta$ ) from positive to negative values could be explained by the high  
388 dominance of negative sites in the  $\text{C}_4\text{A}_3\bar{\text{S}}$  particle surface in contact with citrate. Even though  
389 Bomble's approach is somewhat simplistic because it assumes that all the surfaces have the same  
390 atomic arrangement and that the surface of the grains has the same chemical composition as the bulk,  
391 it gives an interesting insight into the variations of the surface charge with the addition of citric acid.

### 392 3.3. Hydration of CSA model cements containing ye'elimit with two different grain sizes

393 The results of XRD analysis of the hydrated CSA model cements CSA-sol and CSA-chem at  $t_0 = 0$   
394 day, and after curing for 3 days, 7 days and 28 days are shown in Fig. 7a. The corresponding  
395 Rietveld analysis results are given in Table 5. Since we consider that Rietveld analysis gives an  
396 approximate picture of the quantities of remaining reactants (ye'elimit and gypsum) and formed  
397 hydrates, we will focus for clarity on the amount of remaining ye'elimit and on the total quantities

398 of formed hydrates (ettringite, the most abundant hydrate, monosulfoaluminate and gibbsite). The  
399 nature of the formed hydrate phases is in accordance with experimental results previously published  
400 about ye'elimito-calcium sulfate system hydration [32,34–36]. First of all, Fig. 7b displays the  
401 calculated hydration degree,  $\alpha$  given by equation (E.1), of CSA-sol and CSA-chem pastes. After 3  
402 days, CSA-chem paste reaches more than 96.3 % while it is almost 72.4 % for the CSA-sol paste.  
403 After 7 days, the degree of reaction reached 97.6 % and 79.9 % for CSA-chem and CSA-sol,  
404 respectively. Finally, it was observed that at 28 days, the hydration of Ye-chem was nearly complete  
405 reaching almost 98 % hydration degree, while Ye-sol hydration degree attains only 88.7 %.  
406 Concerning the hydrates, the quantities are higher at any time in CSA-chem than in CSA-sol.  
  
407 TGA curves are presented in Fig. 7c. Weight loss between 80 and 150°C can be assigned to ettringite  
408 decomposition (Zone II, Fig. 7c) [27,36]. Gypsum can decompose between 150 and 220°C (Zone III,  
409 Fig. 7c) [27,36]. Weight loss between 100 and 800°C can originate from the decomposition of  
410 monosulfoaluminate (Zones II, III, and IV, Fig. 7c), with a maximum decomposition at 200°C  
411 [27,34]. Lastly, between 200 and 300°C, the weight loss associated to the decomposition of gibbsite  
412 can be detected (Zone IV, Fig. 7c) [27,36]. Despite an overlap between the decomposition of the  
413 different products with temperature, TGA results (Fig. 7c) show higher total weight loss for CSA-  
414 chem compared to CSA-sol, at all hydration durations, which comes mainly from the decomposition  
415 of hydrates. In conclusion, TGA and XRD results give similar trends: the finer the ye'elimito  
416 powder, the faster the cement containing this powder hydrates. The presence of nano-grains of  
417 ye'elimito stimulates nucleation processes during the early cement hydration. The earlier these nuclei  
418 are formed, the earlier they can grow to larger crystals of hydrated phases and thereby accelerates the  
419 cement hydration [17]. Moreover, the high dissolution rate of nano-grains of ye'elimito probably  
420 leads to higher saturation index with respect to the different hydrates during the first days of  
421 hydration [28].

#### 422 3.4. Influence of citric acid on CSA model cements hydration

423 The evolution of phases of the CSA-sol pastes, in the presence of different citric acid dosages (0  
424 wt.%, 0.5 wt.% and 1 wt.%) and for different curing ages (3 days, 7 days and 28 days), were

425 followed by XRD ([Fig. 8a](#)) with the corresponding Rietveld results ([Table 6](#)). Again, we will focus  
426 for clarity on the amount of remaining ye'elimité and on the total quantities of formed hydrates  
427 (ettringite, the most abundant hydrate, monosulfoaluminate and gibbsite). The nature of the formed  
428 hydrate phases is in accordance with experimental results previously published about CSA cement  
429 hydration in the presence citric acid [5,6]. The variations of the calculated hydration degree,  $\alpha$  given  
430 by equation (E.1), of CSA-sol pastes containing different citric acid dosages are presented in [Fig. 8b](#).  
431 The results show that citrate retards the hydration: CSA-sol-0 reacts at a faster pace after 3 days  
432 since the degree of hydration of ye'elimité is 72.4 %, while CSA-sol-0.5 and CSA-sol-1 pastes reach  
433 only 66.6 % and 17.0 %, respectively. After 7 days, CSA-sol-0, CSA-sol-0.5 and CSA-sol-1 reach  
434 more than 79.9 %, almost 73.2 % and 26.4 % degree of hydration, respectively. Lastly, after 28 days  
435 of hydration, the figures are 88.7 %, almost 75.6 % and 65.2 % for CSA-sol-0, CSA-sol-0.5 and  
436 CSA-sol-1 respectively. Therefore, the major effect of citric acid addition on ye'elimité hydration is  
437 the slowing down of the hydration kinetics of the cement paste, suggesting an adsorption of citrate  
438 molecules on ye'elimité grains. In ([section 3-2](#)), it was explained how citric acid can delay ye'elimité  
439 dissolution by the possible citrate adsorption on ye'elimité grains. An analysis of TGA results ([Fig.](#)  
440 [8c](#)) shows the same trend, i.e. a marked decrease of weight loss with the addition of citric acid,  
441 especially with 1 wt.%. The delay induced by citric acid on the reactivity of CSA-sol-0.5 and CSA-  
442 sol-1 can be explained by the fact that citrate molecules will bond with calcium on the surface of  
443 ye'elimité to give a chelate and interfere with ye'elimité dissolution, in addition to forming chelates  
444 with calcium ions already in solution, thus lowering their availability for participating in hydration  
445 reactions as it was already shown for OPC cement [9]. Citric acid addition lowers ettringite  
446 quantities ([Table 6](#)). In fact, some amounts of calcium and aluminium ions produced from ye'elimité  
447 and gypsum dissolution could form chelates with citrate, leading to the decease of the saturation  
448 index with respect to ettringite [28]. The absence of interaction between citrate and ettringite was  
449 proven in literature and it can be confirmed in the present case [8].

450    4. Conclusion

451    In order to contribute to the understanding of CSA concrete characteristics, this work has examined  
452    the effect of fineness on hydration of ye'elmitite powder, which is one component of CSA cements.  
453    Ye'elmitite of two different finesses was prepared either by a solid state method or by a chemical  
454    route. The role of fineness on the hydration of two model CSA cements and the effect of citric acid  
455    addition on the hydration of a CSA model cement were examined. The main conclusions of the  
456    present work can be summarized as follows.

457    The main difference found between the dissolution of ye'elmitite powders prepared by chemical or  
458    solid state routes is related to the reaction rate. The presence of fine grains (100 to 200 nm) of  
459    ye'elmitite accelerates the dissolution. From an industrial point of view, the presence of a fine  
460    fraction of ye'elmitite grains (of the order of 100 – 200 nm) formed after grinding a commercial CSA  
461    clinker can considerably accelerate the hydration and therefore the expansion behavior. The presence  
462    of nano-grains of ye'elmitite stimulates nucleation processes during the early cement hydration. The  
463    earlier these nuclei are formed, the earlier they can develop into large crystals of hydrated phases and  
464    thereby accelerate the cement hydration. Moreover, the high dissolution rate of nano-grains of  
465    ye'elmitite probably leads to higher saturation index with respect to the different hydrates during the  
466    first days of hydration.

467    The addition of citric acid to the mixing water leads to a retarding effect on the dissolution of  
468    ye'elmitite grains. Also, the surface of the grains presents scarce etch pits when citric acid is present  
469    in the water, while the surface seems to be totally attacked with water. These results indicate that the  
470    hydration of CSA model cements prepared from the mixing of ye'elmitite powder – prepared by solid  
471    state reaction - and gypsum is retarded in the presence of citric acid at concentrations of 0.5 wt.%  
472    and 1 wt.% with respect to ye'elmitite. Citric acid may work efficiently as a retarding additive for  
473    CSA cements since it slows down the initial ye'elmitite dissolution. In the present work, it was also  
474    shown that the addition of citric acid with CSA model cements delays the formation of hydrates,  
475    especially ettringite. The delay effect of citric acid can be explained by the fact that citrate molecules

476 form chelates with calcium on the surface of ye'elimite and interfere with ye'elimite dissolution, in  
477 addition to forming chelates with calcium ions already in solution, thus lowering their availability for  
478 participating in hydration reactions.

479 Expansion behavior of commercial CSA cements could be controlled by the addition of citric acid,  
480 because it is well known that the fresh CSA concrete properties depend mainly on ettringite  
481 quantities in the hydrated cement pastes.

482 In conclusion, powder fineness and citric acid addition are two levers that could be helpful for  
483 industrial CSA cement producers, because they constitute a practical way to control the amount of  
484 formed ettringite, and hence the expansion behaviour of CSA cements. The influence of ye'elimite  
485 powder fineness and citric acid addition on the dimensional stability, workability, mechanical  
486 properties and durability performances of CSA cements and concretes could be the subject of further  
487 studies.

488 [References](#)

- 489 [1] F.P. Glasser, L. Zhang, High-performance cement matrices based on calcium sulfoaluminate–  
490 belite compositions, *Cem. Concr. Res.* 31 (2001) 1881–1886.
- 491 [2] R. Trauchessec, J.-M. Mechling, A. Lecomte, A. Roux, B. Le Rolland, Hydration of ordinary  
492 Portland cement and calcium sulfoaluminate cement blends, *Cem. Concr. Compos.* 56 (2015)  
493 106–114.
- 494 [3] M.C.G. Juenger, F. Winnefeld, J.L. Provis, J.H. Ideker, Advances in alternative cementitious  
495 binders, *Cem. Concr. Res.* 41 (2011) 1232–1243.
- 496 [4] L.E. Burris, K.E. Kurtis, Influence of set retarding admixtures on calcium sulfoaluminate  
497 cement hydration and property development, *Cem. Concr. Res.* 104 (2018) 105–113.
- 498 [5] J. Tinnea, J.F. Young, Influence of Citric Acid on Reactions in the System 3CaO·Al<sub>2</sub>O<sub>3</sub>–  
499 CaSO<sub>4</sub>·2H<sub>2</sub>O–CaO–H<sub>2</sub>O, *J. Am. Ceram. Soc.* 60 (1977) 387–389.  
500 <https://doi.org/10.1111/j.1151-2916.1977.tb15518.x>.
- 501 [6] F. Winnefeld, S. Klemm, Influence of citric acid on the hydration kinetics of calcium  
502 sulfoaluminate cement, in: Submitt. First Int. Conf. Sulphoaluminate Cem. Mater. Eng.  
503 Technol. Wuhan China, 2013.
- 504 [7] M. Zajac, J. Skocek, F. Bullerjahn, M. Ben Haha, Effect of retarders on the early hydration of  
505 calcium-sulpho-aluminate (CSA) type cements, *Cem. Concr. Res.* 84 (2016) 62–75.  
506 <https://doi.org/10.1016/j.cemconres.2016.02.014>.
- 507 [8] A.M. Cody, H. Lee, R.D. Cody, P.G. Spry, The effects of chemical environment on the  
508 nucleation, growth, and stability of ettringite [Ca<sub>3</sub>Al(OH)<sub>6</sub>]<sub>2</sub>(SO<sub>4</sub>)<sub>3</sub>·26H<sub>2</sub>O, *Cem. Concr.*  
509 *Res.* 34 (2004) 869–881.
- 510 [9] M. Prisciandaro, A. Lancia, D. Musmarra, The retarding effect of citric acid on calcium sulfate  
511 nucleation kinetics, *Ind. Eng. Chem. Res.* 42 (2003) 6647–6652.

- 512 [10] J.-B. Champenois, M. Dhoury, C.C.D. Coumes, C. Mercier, B. Revel, P. Le Bescop, D. Damidot,  
513 Influence of sodium borate on the early age hydration of calcium sulfoaluminate cement,  
514 *Cem. Concr. Res.* 70 (2015) 83–93.
- 515 [11] G. Zhang, G. Li, Y. Li, Effects of superplasticizers and retarders on the fluidity and strength of  
516 sulphaaluminate cement, *Constr. Build. Mater.* 126 (2016) 44–54.
- 517 [12] F. Sajedi, H.A. Razak, Effects of curing regimes and cement fineness on the compressive  
518 strength of ordinary Portland cement mortars, *Constr. Build. Mater.* 25 (2011) 2036–2045.
- 519 [13] E.H. Kadri, S. Aggoun, G. De Schutter, K. Ezziane, Combined effect of chemical nature and  
520 fineness of mineral powders on Portland cement hydration, *Mater. Struct.* 43 (2010) 665–673.
- 521 [14] E.C. Higginson, The effect of cement fineness on concrete, in: *Fineness Cem.*, ASTM  
522 International, 1970.
- 523 [15] K.M. Alexander, The relationship between strength and the composition and fineness of  
524 cement, *Cem. Concr. Res.* 2 (1972) 663–680.
- 525 [16] J. Hu, Z. Ge, K. Wang, Influence of cement fineness and water-to-cement ratio on mortar  
526 early-age heat of hydration and set times, *Constr. Build. Mater.* 50 (2014) 657–663.
- 527 [17] G. Land, D. Stephan, Controlling cement hydration with nanoparticles, *Cem. Concr. Compos.*  
528 57 (2015) 64–67.
- 529 [18] J.-T. Song, J.F. Young, Direct synthesis and hydration of calcium aluminosulfate ( $\text{Ca}_4\text{Al}_6\text{O}_{16}\text{S}$ ),  
530 *J. Am. Ceram. Soc.* 85 (2002) 535–539.
- 531 [19] J.J. Thomas, S. Ghazizadeh, E. Masoero, Kinetic mechanisms and activation energies for  
532 hydration of standard and highly reactive forms of  $\beta$ -dicalcium silicate (C2S), *Cem. Concr. Res.*  
533 100 (2017) 322–328.
- 534 [20] H. Pöllmann, *Cementitious Materials: Composition, Properties, Application*, Walter de Gruyter  
535 GmbH & Co KG, 2017.
- 536 [21] S.-H. Hong, J.F. Young, Hydration kinetics and phase stability of dicalcium silicate synthesized  
537 by the Pechini process, *J. Am. Ceram. Soc.* 82 (1999) 1681–1686.
- 538 [22] D.A. Fumo, M.R. Morelli, A.M. Segadaes, Combustion synthesis of calcium aluminates, *Mater.  
539 Res. Bull.* 31 (1996) 1243–1255.
- 540 [23] P.K. Mehta, Mechanism of expansion associated with ettringite formation, *Cem. Concr. Res.* 3  
541 (1973) 1–6.
- 542 [24] K. Ogawa, D.M. Roy, C4A3S hydration ettringite formation, and its expansion mechanism: I.  
543 expansion; Ettringite stability, *Cem. Concr. Res.* 11 (1981) 741–750.
- 544 [25] Y. El Khessaimi, Y. El Hafiane, A. Smith, R. Trauchessec, C. Diliberto, A. Lecomte, Solid-state  
545 synthesis of pure ye'elimité, *J. Eur. Ceram. Soc.* 38 (2018) 3401–3411.
- 546 [26] H. Le Chatelier, *Recherches expérimentales sur la constitution des mortiers hydrauliques*,  
547 Dunod, 1904.
- 548 [27] F. Winnefeld, S. Barlag, Calorimetric and thermogravimetric study on the influence of calcium  
549 sulfate on the hydration of ye'elimité, *J. Therm. Anal. Calorim.* 101 (2009) 949–957.
- 550 [28] F. Winnefeld, B. Lothenbach, Hydration of calcium sulfoaluminate cements—experimental  
551 findings and thermodynamic modelling, *Cem. Concr. Res.* 40 (2010) 1239–1247.
- 552 [29] R. Trauchessec, J.-M. Mechling, A. Lecomte, A. Roux, B. Le Rolland, Impact of anhydrite  
553 proportion in a calcium sulfoaluminate cement and Portland cement blend, *Adv. Cem. Res.* 26  
554 (2014) 325–333.
- 555 [30] F. Hanic, I. Kaprálik, A. Gabrisová, Mechanism of hydration reactions in the system  $\text{C}_4\text{A}_3\text{S} \square$   
556  $\text{CS} \square \text{CaO} \square \text{H}_2\text{O}$  referred to hydration of sulphaaluminate cements, *Cem. Concr. Res.* 19 (1989)  
557 671–682.
- 558 [31] C.W. Hargis, A.P. Kirchheim, P.J. Monteiro, E.M. Gartner, Early age hydration of calcium  
559 sulfoaluminate (synthetic ye'elimité, C4A3S) in the presence of gypsum and varying amounts  
560 of calcium hydroxide, *Cem. Concr. Res.* 48 (2013) 105–115.

- 561 [32] F. Bullerjahn, E. Boehm-Courjault, M. Zajac, M. Ben Haha, K. Scrivener, Hydration reactions  
562 and stages of clinker composed mainly of stoichiometric ye'elimitite, *Cem. Concr. Res.* 116  
563 (2019) 120–133. <https://doi.org/10.1016/j.cemconres.2018.10.023>.
- 564 [33] M. Zajac, J. Skocek, F. Bullerjahn, B. Lothenbach, K. Scrivener, M.B. Haha, Early hydration of  
565 ye'elimitite: Insights from thermodynamic modelling, *Cem. Concr. Res.* 120 (2019) 152–163.
- 566 [34] A. Cuesta, G. Álvarez-Pinazo, S.G. Sanfélix, I. Peral, M.A. Aranda, A.G. De la Torre, Hydration  
567 mechanisms of two polymorphs of synthetic ye'elimitite, *Cem. Concr. Res.* 63 (2014) 127–136.
- 568 [35] D. Jansen, A. Spies, J. Neubauer, D. Ectors, F. Goetz-Neunhoeffer, Studies on the early  
569 hydration of two modifications of ye'elimitite with gypsum, *Cem. Concr. Res.* 91 (2017) 106–  
570 116.
- 571 [36] F. Bullerjahn, M. Zajac, M.B. Haha, K.L. Scrivener, Factors influencing the hydration kinetics of  
572 ye'elimitite; effect of mayenite, *Cem. Concr. Res.* 116 (2019) 113–119.
- 573 [37] C.W. Hargis, A. Telesca, P.J.M. Monteiro, Calcium sulfoaluminate (Ye'elimitite) hydration in the  
574 presence of gypsum, calcite, and vaterite, *Cem. Concr. Res.* 65 (2014) 15–20.  
575 <https://doi.org/10.1016/j.cemconres.2014.07.004>.
- 576 [38] M.B. Haha, F. Winnefeld, A. Pisch, Advances in understanding ye'elimitite-rich cements, *Cem.*  
577 *Concr. Res.* 123 (2019) 105778.
- 578 [39] Y. El Khessaimi, Y. El Hafiane, A. Smith, Ye'elimitite synthesis by chemical routes, *J. Eur. Ceram.*  
579 *Soc.* 39 (2019) 1683–1695.
- 580 [40] X. Li, Y. Zhang, X. Shen, Q. Wang, Z. Pan, Kinetics of calcium sulfoaluminate formation from  
581 tricalcium aluminate, calcium sulfate and calcium oxide, *Cem. Concr. Res.* 55 (2014) 79–87.
- 582 [41] A. Cuesta, A.G. De la Torre, I. Santacruz, P. Trtik, J.C. Da Silva, A. Diaz, M. Holler, M.A. Aranda,  
583 Chemistry and mass density of aluminum hydroxide gel in eco-cements by ptychographic x-  
584 ray computed tomography, *J. Phys. Chem. C.* 121 (2017) 3044–3054.
- 585 [42] Y. El Khessaimi, Y. El Hafiane, A. Smith, Examination of ye'elimitite formation mechanisms, *J.*  
586 *Eur. Ceram. Soc.* 39 (2019) 5086–5095.
- 587 [43] Á.G. De la Torre, I. Santacruz, L. León-Reina, A. Cuesta, M.A.G. Aranda, 1. Diffraction and  
588 crystallography applied to anhydrous cements, in: H. Pöllmann (Ed.), *Cem. Mater.*, De Gruyter,  
589 Berlin, Boston, 2017: pp. 3–30. doi:10.1515/9783110473728-002., in: n.d.
- 590 [44] A. Cuesta, A.G. De la Torre, E.R. Losilla, V.K. Peterson, P. Rejmak, A. Ayuela, C. Frontera, M.A.  
591 Aranda, Structure, atomistic simulations, and phase transition of stoichiometric yeelimitite,  
592 *Chem. Mater.* 25 (2013) 1680–1687.
- 593 [45] F. Goetz-Neunhoeffer, J. Neubauer, Refined ettringite ( $\text{Ca}_6\text{Al}_2(\text{SO}_4)_3(\text{OH})_{12}\cdot 26\text{H}_2\text{O}$ )  
594 structure for quantitative X-ray diffraction analysis, *Powder Diffr.* 21 (2006) 4–11.
- 595 [46] R. Allmann, Refinement of the hybrid layer structure  $[\text{Ca}_2\text{Al}(\text{OH})_6]^+ \cdot [\text{1/2SO}_4 \cdot 3\text{H}_2\text{O}]^-$ , *Neues*  
596 *Jahrb. Für Mineral. Monatshefte.* 1977 (1977) 136–143.
- 597 [47] H. Saalfeld, M. Wedde, Refinement of the crystal structure of gibbsite,  $\text{A}_1(\text{OH})_3$ , *Z. Für Krist.-*  
598 *Cryst. Mater.* 139 (1974) 129–135.
- 599 [48] G. Angeles, M.-G. López-Olmo, C. Alvarez-Rua, S. García-Granda, M.A. Aranda, Structure and  
600 microstructure of gypsum and its relevance to Rietveld quantitative phase analyses, *Powder*  
601 *Diffr.* 19 (2004) 240–246.
- 602 [49] B.H. Toby, R factors in Rietveld analysis: how good is good enough?, *Powder Diffr.* 21 (2006)  
603 67–70.
- 604 [50] A. Cuesta, A.G. De la Torre, I. Santacruz, P. Trtik, J.C. Da Silva, A. Diaz, M. Holler, M.A. Aranda,  
605 Chemistry and mass density of aluminum hydroxide gel in eco-cements by ptychographic x-  
606 ray computed tomography, *J. Phys. Chem. C.* 121 (2017) 3044–3054.
- 607 [51] G. Álvarez-Pinazo, A. Cuesta, M. García-Maté, I. Santacruz, E.R. Losilla, A.G. De la Torre, L.  
608 León-Reina, M.A. Aranda, Rietveld quantitative phase analysis of Yeelimitite-containing  
609 cements, *Cem. Concr. Res.* 42 (2012) 960–971.
- 610 [52] R. Trauchessec, *Mélanges de ciments sulfoalumineux et Portland*, PhD Thesis, Université de  
611 Lorraine, 2013.

- 612 [53] L. Pelletier, F. Winnefeld, B. Lothenbach, The ternary system Portland cement–calcium  
613 sulfoaluminate clinker–anhydrite: hydration mechanism and mortar properties, *Cem. Concr.*  
614 *Compos.* 32 (2010) 497–507.
- 615 [54] W. Hanley, D. Constantiner, J. Goldbrunner, Retarder for calcium sulfoaluminate cements,  
616 2004.
- 617 [55] T. EN, 196-1. Methods of testing cement—Part 1: Determination of strength, *Eur. Comm.*  
618 *Stand.* 26 (2005).
- 619 [56] P. Juillard, E. Gallucci, R. Flatt, K. Scrivener, Dissolution theory applied to the induction period  
620 in alite hydration, *Cem. Concr. Res.* 40 (2010) 831–844.  
621 <https://doi.org/10.1016/j.cemconres.2010.01.012>.
- 622 [57] P. Juillard, E. Gallucci, Morpho-topological investigation of the mechanisms and kinetic  
623 regimes of alite dissolution, *Cem. Concr. Res.* 76 (2015) 180–191.  
624 <https://doi.org/10.1016/j.cemconres.2015.06.001>.
- 625 [58] L. Nicoleau, A. Nonat, D. Perrey, The di- and tricalcium silicate dissolutions, *Cem. Concr. Res.*  
626 47 (2013) 14–30. <https://doi.org/10.1016/j.cemconres.2013.01.017>.
- 627 [59] P. Barret, D. Ménétrier, Filter dissolution of C3S as a function of the lime concentration in a  
628 limited amount of lime water, *Cem. Concr. Res.* 10 (1980) 521–534.
- 629 [60] A.C. Lasaga, A. Luttge, Variation of crystal dissolution rate based on a dissolution stepwave  
630 model, *Science.* 291 (2001) 2400–2404.
- 631 [61] P.M. Dove, N. Han, Kinetics of mineral dissolution and growth as reciprocal microscopic  
632 surface processes across chemical driving force, in: *AIP Conf. Proc.*, AIP, 2007: pp. 215–234.
- 633 [62] P.M. Dove, N. Han, J.J. De Yoreo, Mechanisms of classical crystal growth theory explain quartz  
634 and silicate dissolution behavior, *Proc. Natl. Acad. Sci.* 102 (2005) 15357–15362.
- 635 [63] A.C. Lasaga, *Kinetic theory in the earth sciences*, Princeton university press, 2014.
- 636 [64] T.E. Burch, K.L. Nagy, A.C. Lasaga, Free energy dependence of albite dissolution kinetics at  
637 80°C and pH 8.8, *Chem. Geol.* 105 (1993) 137–162. [https://doi.org/10.1016/0009-2541\(93\)90123-Z](https://doi.org/10.1016/0009-2541(93)90123-Z).
- 639 [65] R.N. Goldberg, N. Kishore, R.M. Lennen, Thermodynamic quantities for the ionization  
640 reactions of buffers, *J. Phys. Chem. Ref. Data.* 31 (2002) 231–370.
- 641 [66] D.B. Emmert, P.J. Stoehr, G. Stoesser, G.N. Cameron, The European bioinformatics institute  
642 (EBI) databases, *Nucleic Acids Res.* 22 (1994) 3445–3449.
- 643 [67] A. Cuesta, A.G. De la Torre, E.R. Losilla, V.K. Peterson, P. Rejmak, A. Ayuela, C. Frontera,  
644 M.A.G. Aranda, Structure, Atomistic Simulations, and Phase Transition of Stoichiometric  
645 Yeelimite, *Chem. Mater.* 25 (2013) 1680–1687. <https://doi.org/10.1021/cm400129z>.
- 646 [68] J.-P. Boisvert, M. Domenech, A. Foissy, J. Persello, J.-C. Mutin, Hydration of calcium sulfate  
647 hemihydrate ( $\text{CaSO}_4 \cdot 12\text{H}_2\text{O}$ ) into gypsum ( $\text{CaSO}_4 \cdot 2\text{H}_2\text{O}$ ). The influence of the sodium poly  
648 (acrylate)/surface interaction and molecular weight, *J. Cryst. Growth.* 220 (2000) 579–591.
- 649 [69] A. Ersen, A. Smith, T. Chotard, Effect of malic and citric acid on the crystallisation of gypsum  
650 investigated by coupled acoustic emission and electrical conductivity techniques, *J. Mater. Sci.*  
651 41 (2006) 7210–7217.
- 652 [70] E. Badens, S. Veesler, R. Boistelle, Crystallization of gypsum from hemihydrate in presence of  
653 additives, *J. Cryst. Growth.* 198–199 (1999) 704–709. [https://doi.org/10.1016/S0022-0248\(98\)01206-8](https://doi.org/10.1016/S0022-0248(98)01206-8).
- 655 [71] J.P. Bombed, Rhéologie des mortiers et des bétons frais, influence du facteur ciment, in:  
656 Proceeding RILEM Leeds Semin., 1973: pp. 1–169.
- 657 [72] A. Smith, Y. El Hafiane, J.-P. Bonnet, P. Quintard, B. Tanouti, Role of a small addition of acetic  
658 acid on the setting behavior and on the microstructure of a calcium aluminate cement, *J. Am.*  
659 *Ceram. Soc.* 88 (2005) 2079–2084.

## Figure captions

Figure 1	(a) Calculated ye'elimit hydration degree ( $\alpha\%$ ); Formed hydrates quantities relevant to Ettringite (b), Monosulfoaluminate (c) and Gibbsite (d); "w/c" refers to water by cement weight ratio; References: Cuesta et al.,2014 [34], Hargis et al.,2014 [37], Jansen et al.,2017 [35], Bullerjahn et al.,2019 [36], ( $\alpha\%$ ) is given by equation (E.1).
Figure 2	Preparation protocol ye'elimit dissolution study of suspensions, (a) based on Ye-sol or Ye-chem, (b) based on Ye-sol with different citric acid percentages (0 wt.%, 5 wt.% and 10 wt.%).
Figure 3	Preparation protocol for hydration study of CSA model cement pastes, (a) based on Ye-sol or Ye-chem (blended with gypsum), or (b) based on Ye-sol (blended with gypsum) with different citric acid percentages (0 wt%, 0.5 wt.% and 1 wt.%).
Figure 4	(a) Ionic conductivity evolution of ye'elimit suspensions Ye-sol-0, Ye-chem, Ye-sol-5 and Ye-sol-10. All suspensions were prepared with w/c = 1000. t = 0 min in the graph's abscissa refers to the time when ye'elimit is added to the citric acid solution. (b) Ionic conductivity evolution of gypsum suspensions with different citric acid additions: 0 wt.% (Gy-0), 5 wt.% (Gy-5) and 10 wt.% (Gy-10). All suspensions were prepared with w/c = 1000. t = 0 min in the graph's abscissa refers to the time when gypsum is added to the citric acid solution.
Figure 5	SEM micrographs of Ye-sol-0 (a), Ye-sol-10 (b) and Ye-chem (c) suspensions. Observations were carried out after 1 min of hydration and all suspensions were prepared with W/C = 1000.
Figure 6	(a) Citric acid structure (CHEBI:30769) from the European Bioinformatics Institute Database [66], atoms are represented as spheres and are color coded as: carbon (grey), hydrogen (white) and oxygen (red). (b) Orthorhombic ye'elimit structure from Cuesta et al. [67] showing the (13 $\bar{1}$ ) crystallographic plane, Ca denoted within dark-green spheres, Al within light blue

	tetrahedra, S within yellow tetrahedra, and O are red, for clarity CaO bonds are omitted in the represented structure.
Figure 7	XRD patterns (a), calculated hydration degree ( $\alpha$ ) (b), for CSA model cements (CSA-sol-0) and (CSA-Chem) at different hydration ages. E: ettringite; G: Gypsum; M: monosulfate; Y: ye'elimit; A: Gibssite, ( $\alpha\%$ ) is given by equation (E.1), and TGA curves (c).
Figure 8	XRD patterns (a), calculated hydration degree ( $\alpha$ ) (b), for CSA model cements (CSA-sol-0), (CSA-sol-0.5) and (CSA-sol-1) at different hydration ages. E: ettringite; G: Gypsum; M: monosulfate; Y: ye'elimit; A: Gibssite. ( $\alpha\%$ ) is given by equation (E.1), and TGA curves (c).

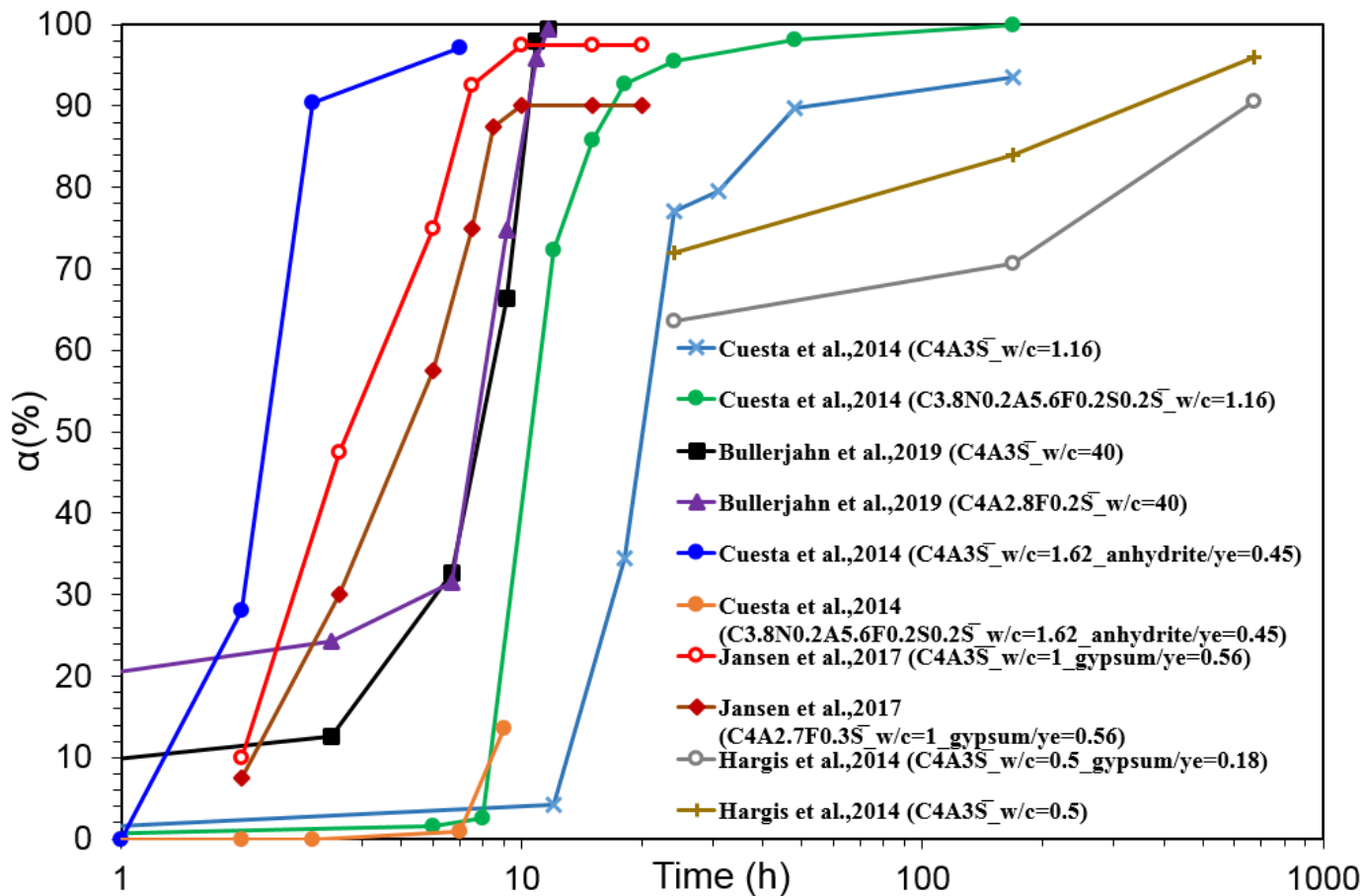


Figure 1-(a)

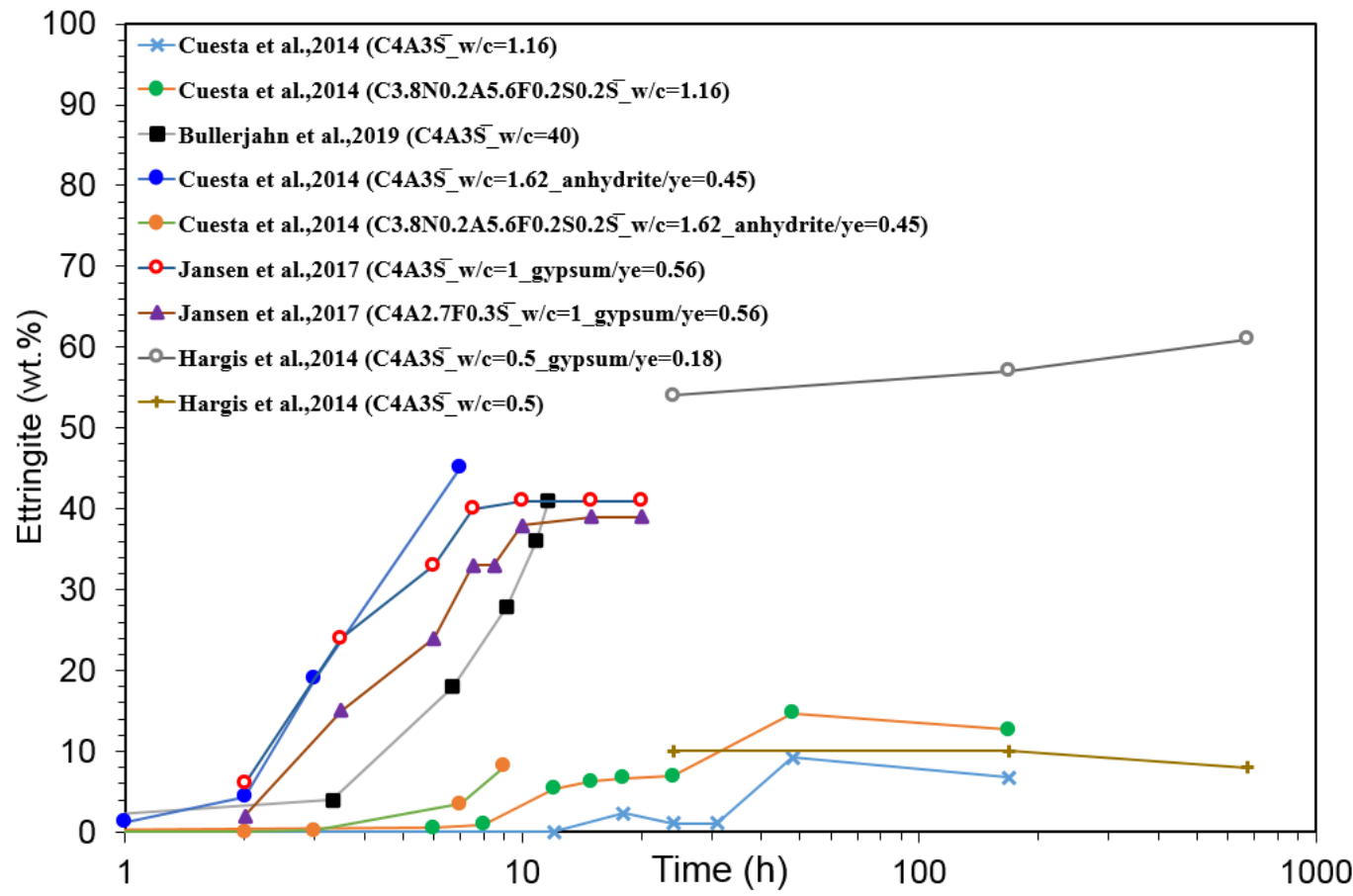


Figure 1-(b)

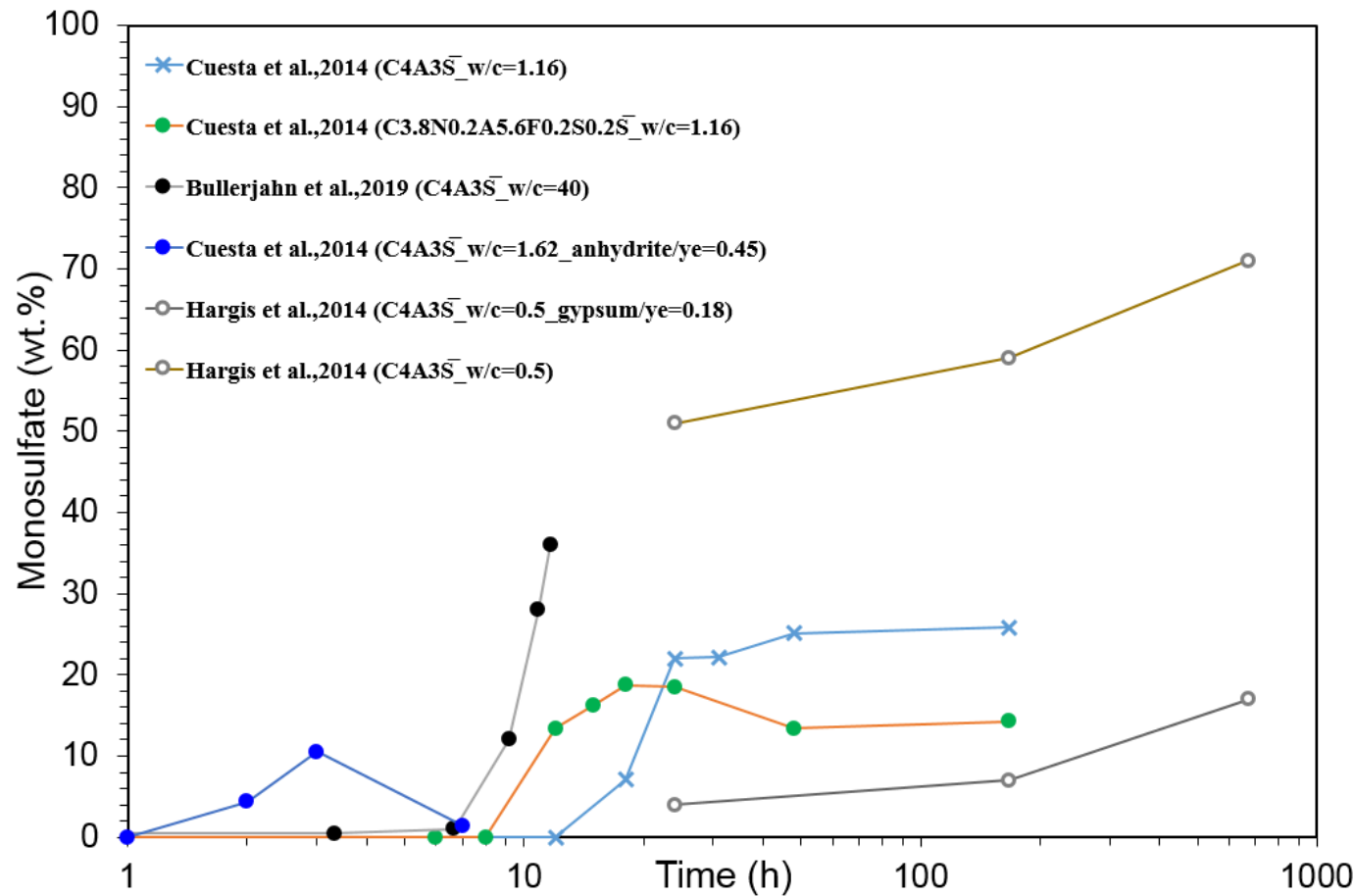


Figure 1-(c)

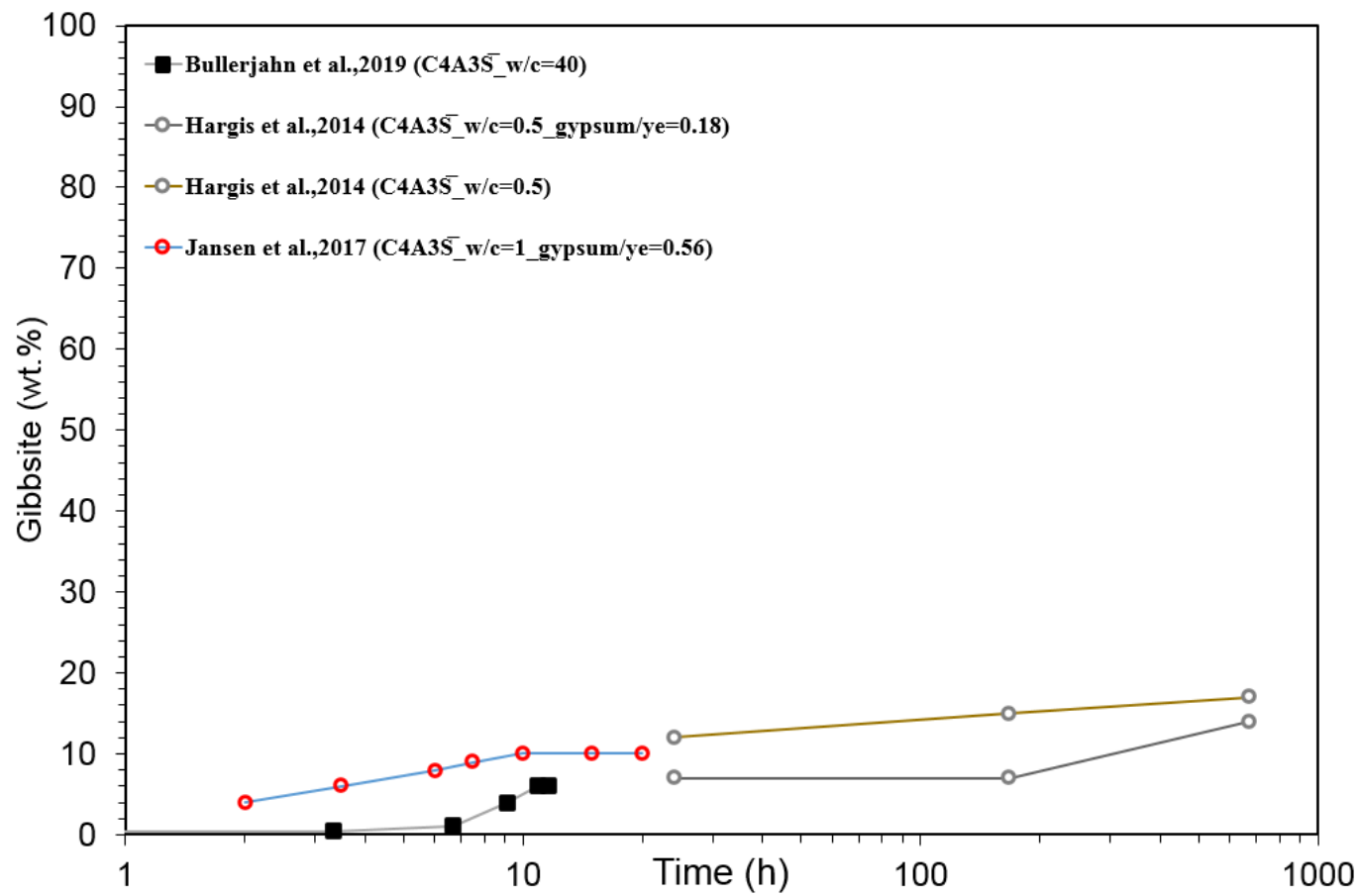


Figure 1-(d)

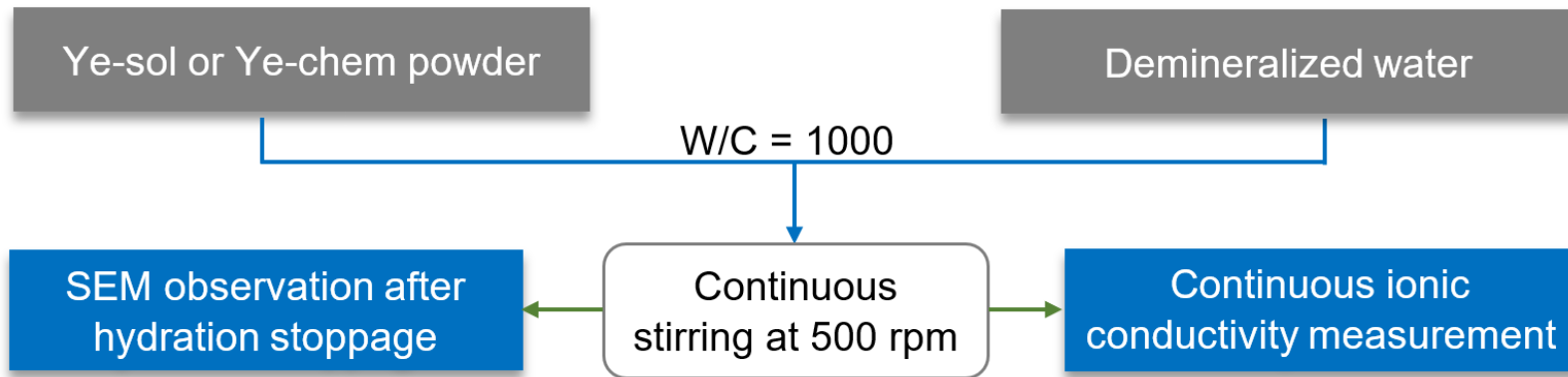


Figure 2a

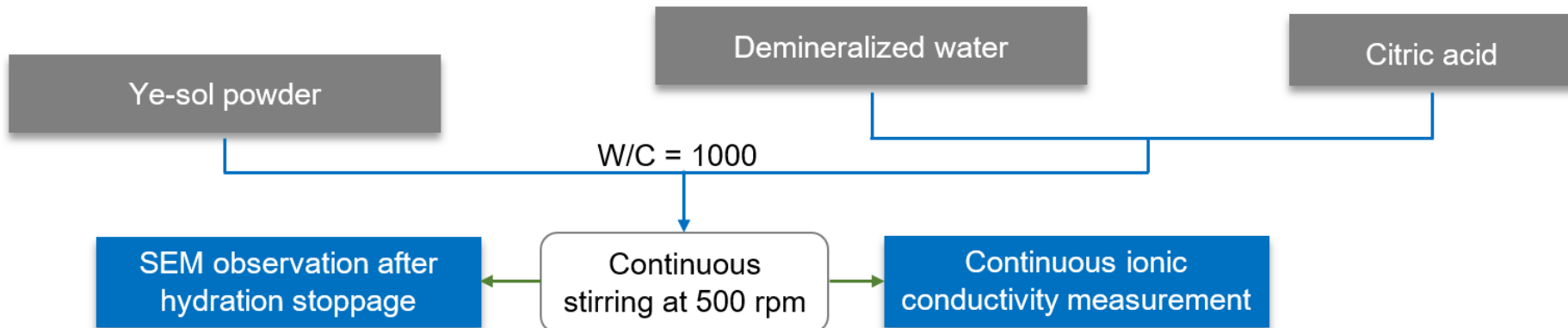


Figure 2b

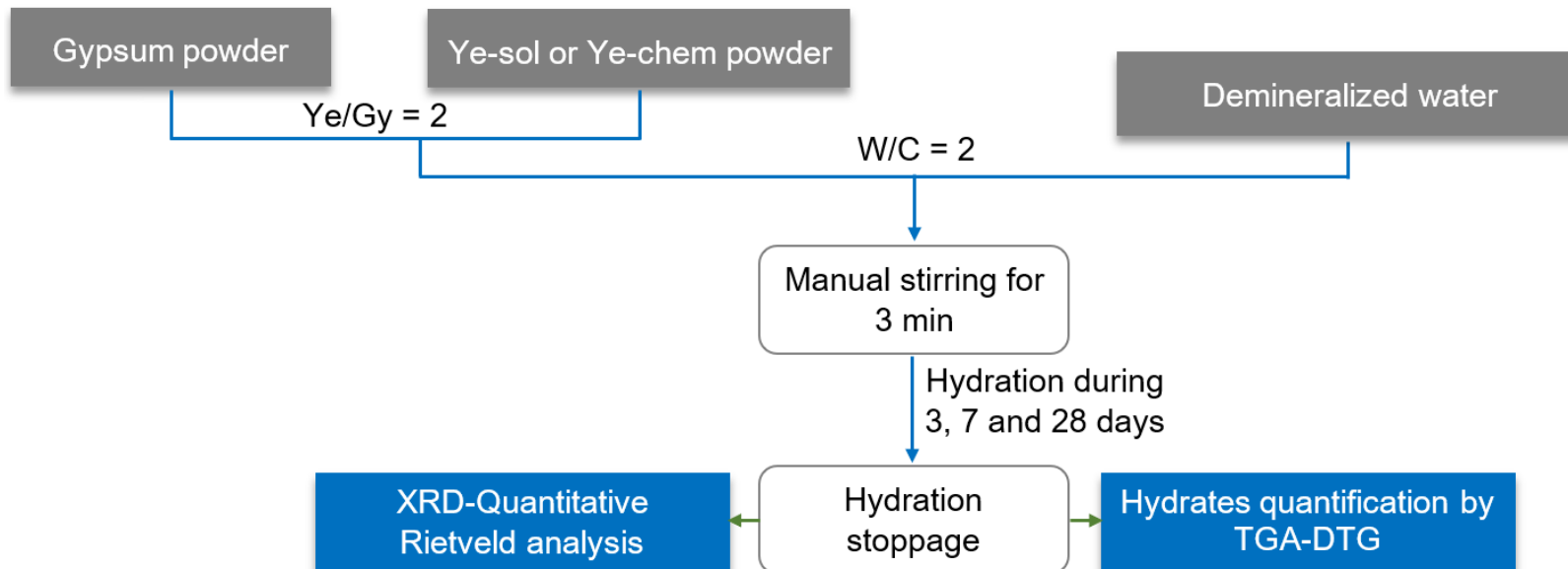


Figure 3a

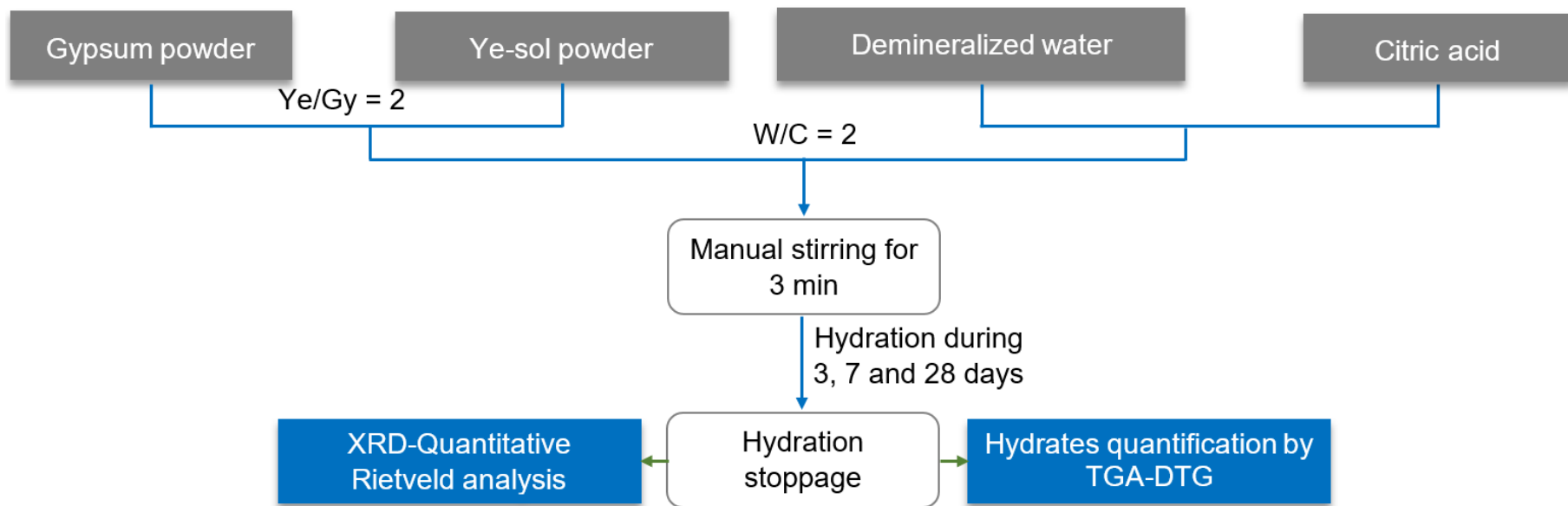


Figure 3b

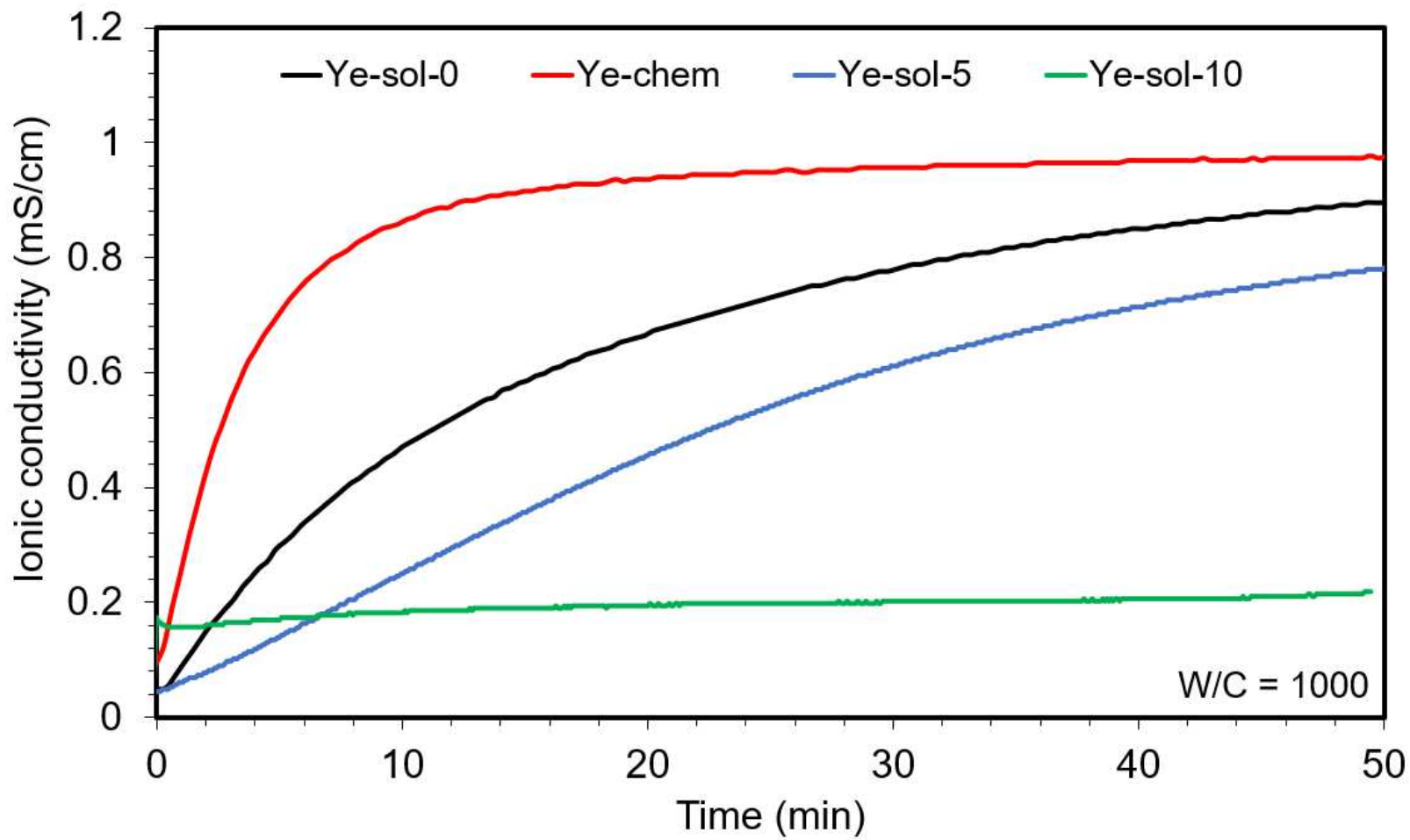


Figure 4a

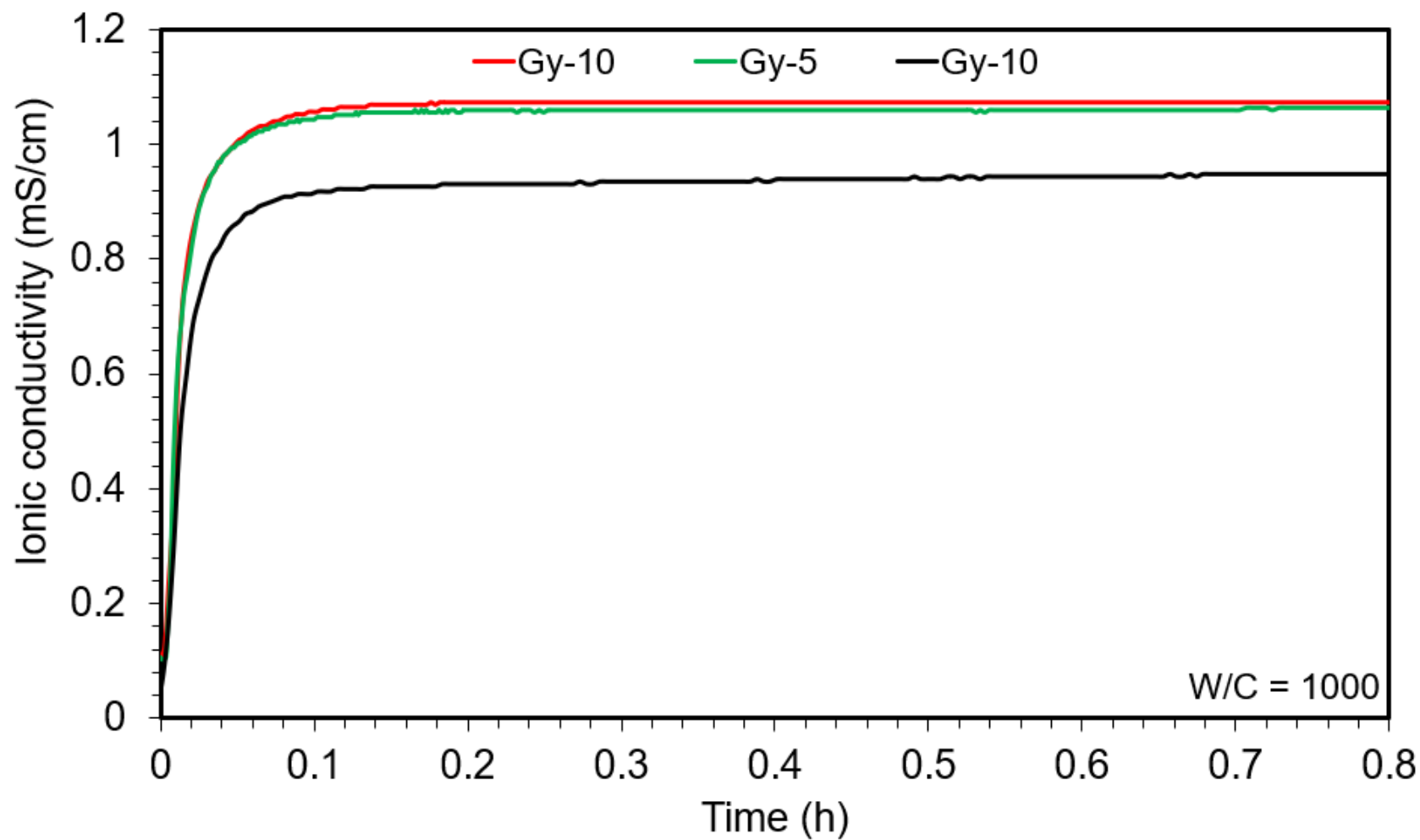
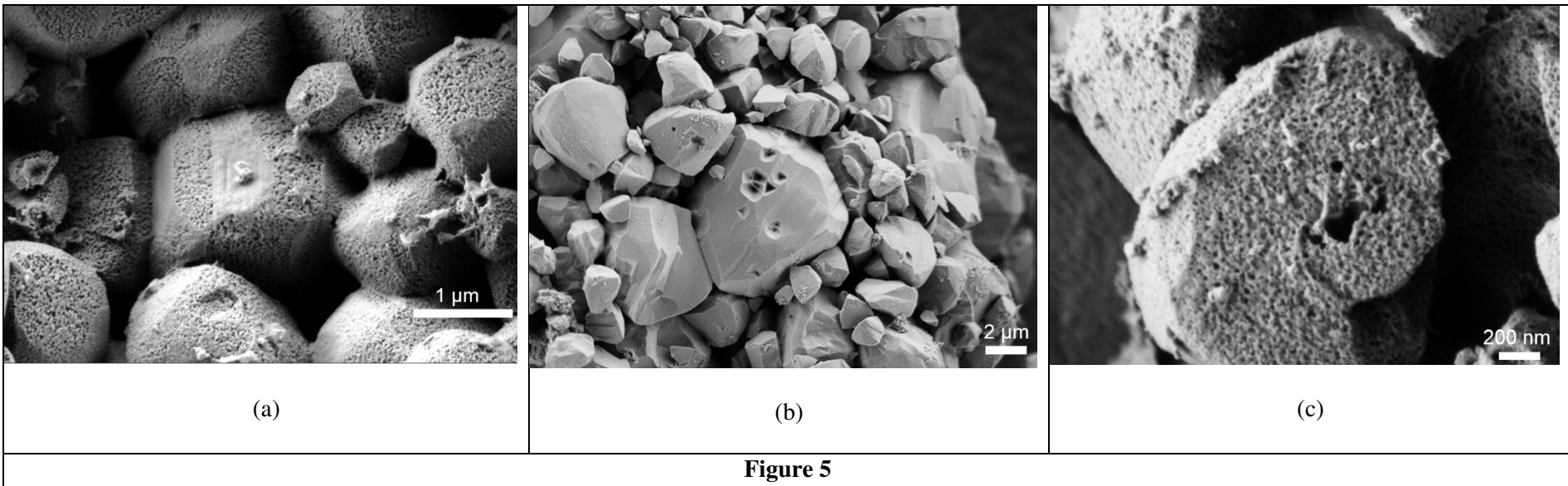
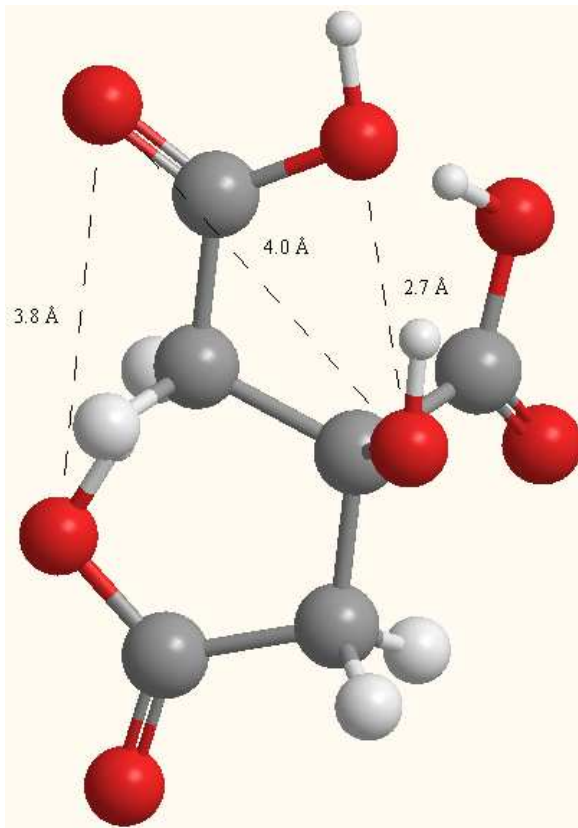


Figure 4b



**Figure 5**



**Figure 6 - (a)**

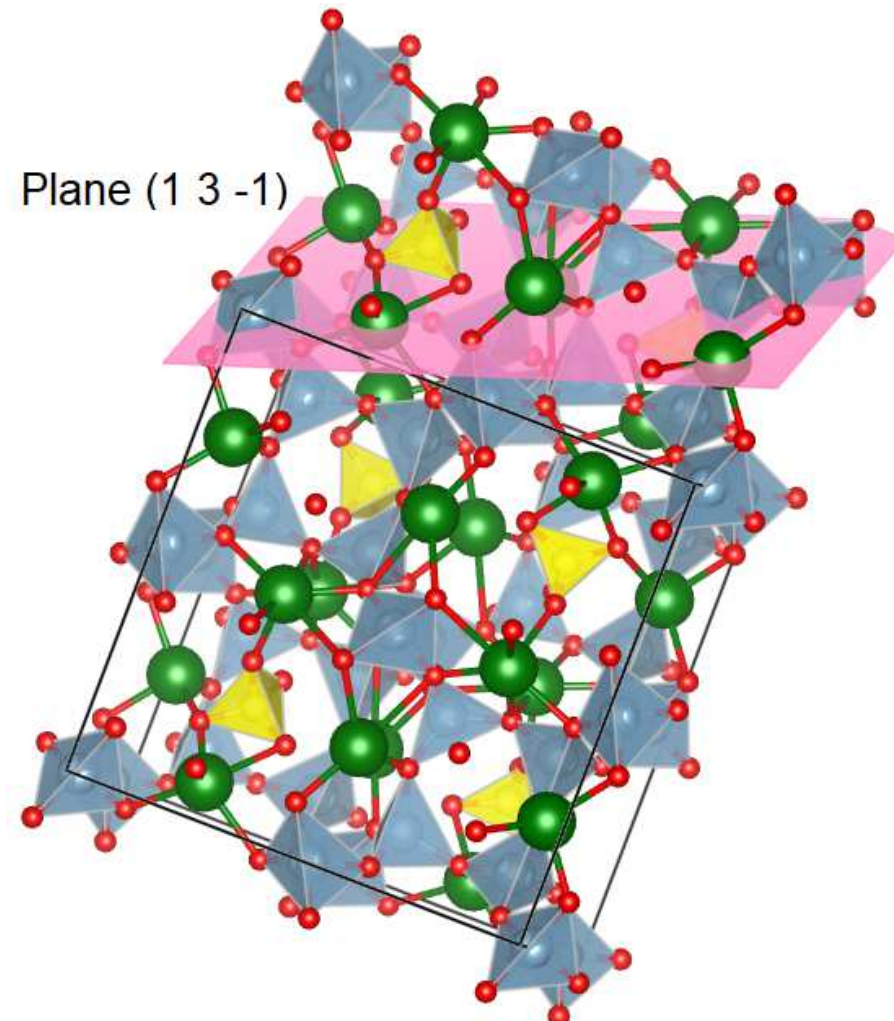


Figure 6 - (b)

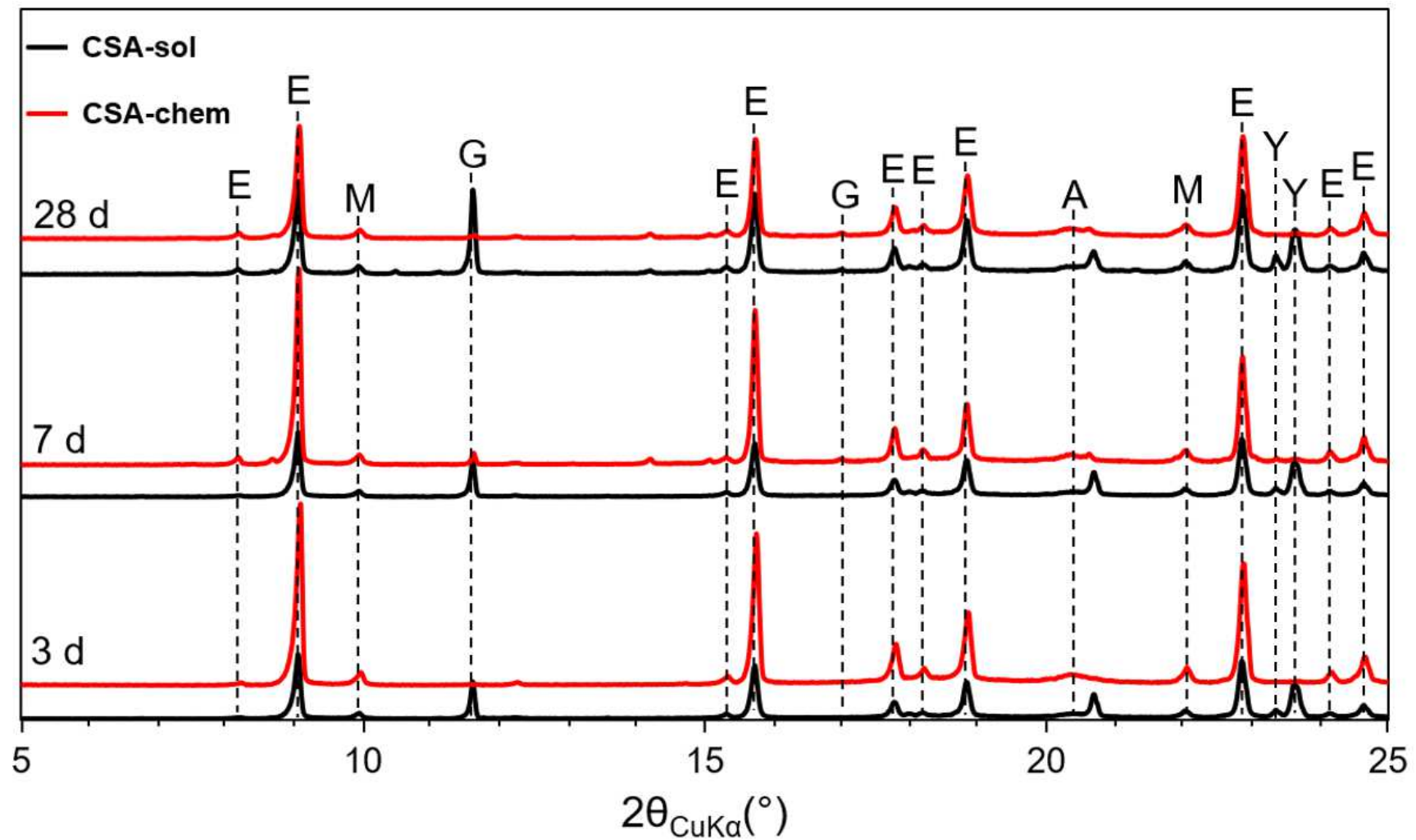
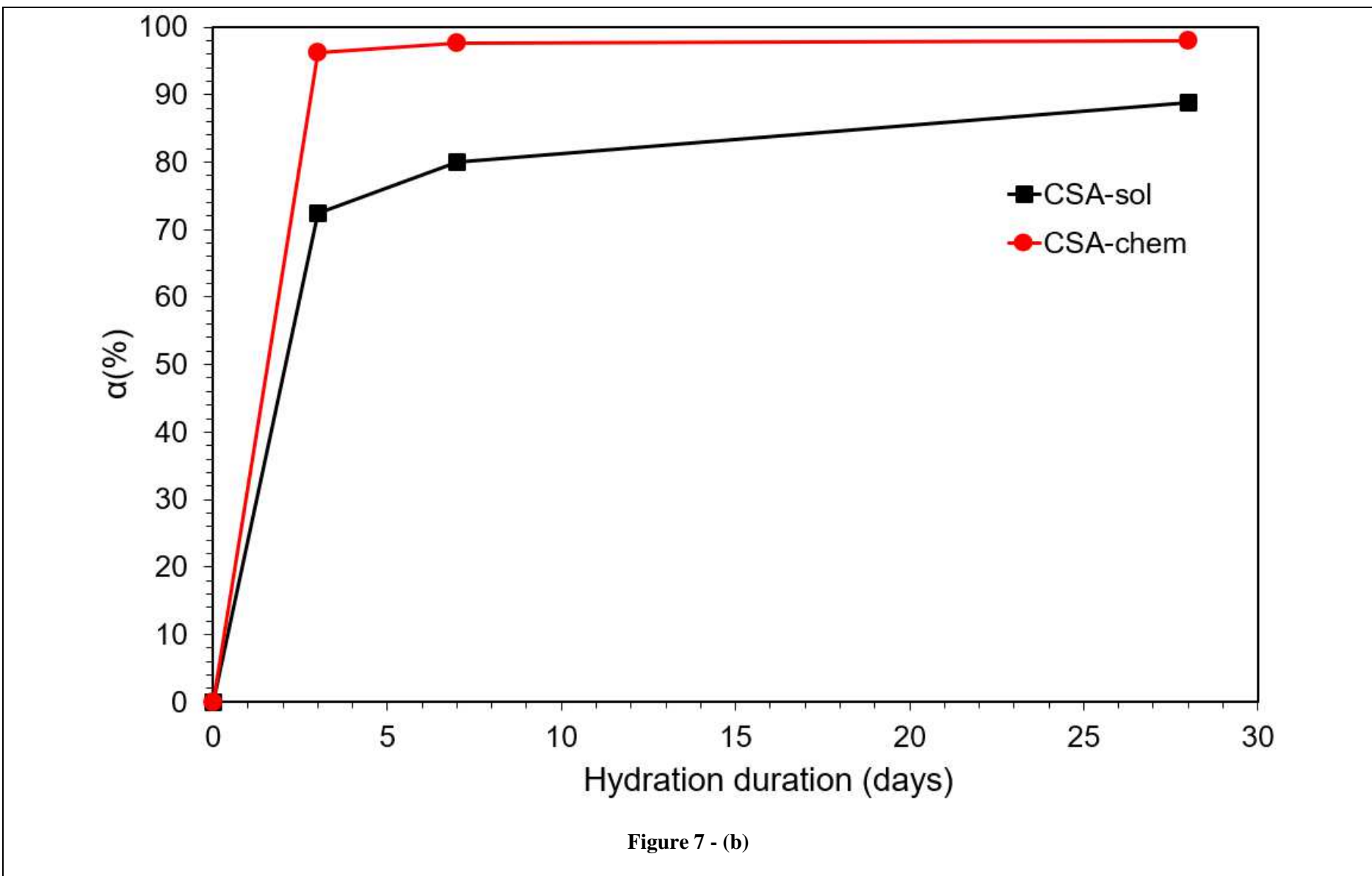
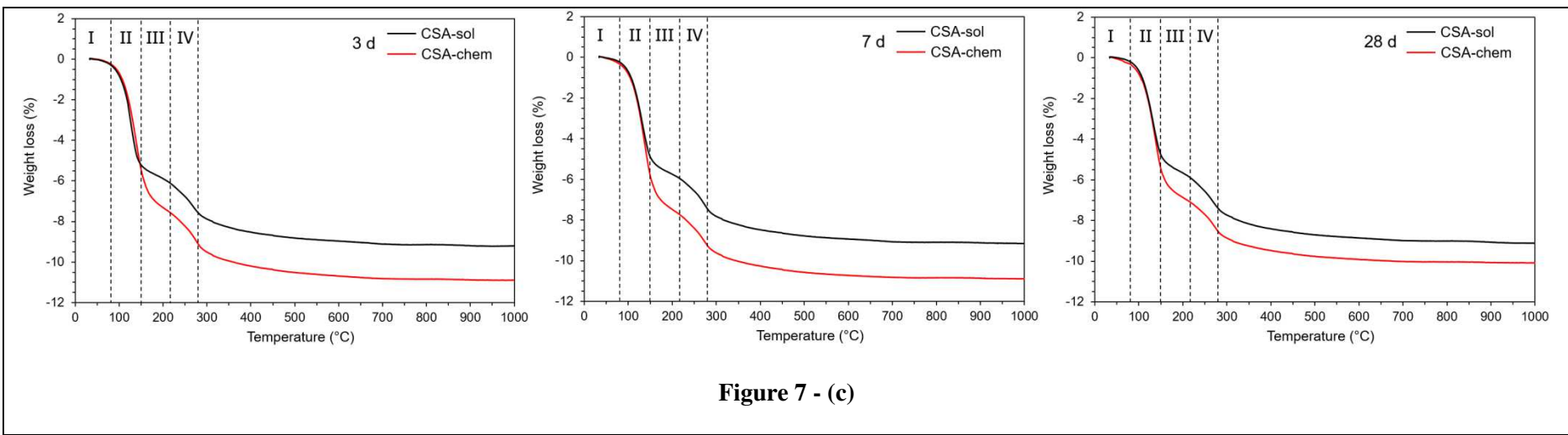
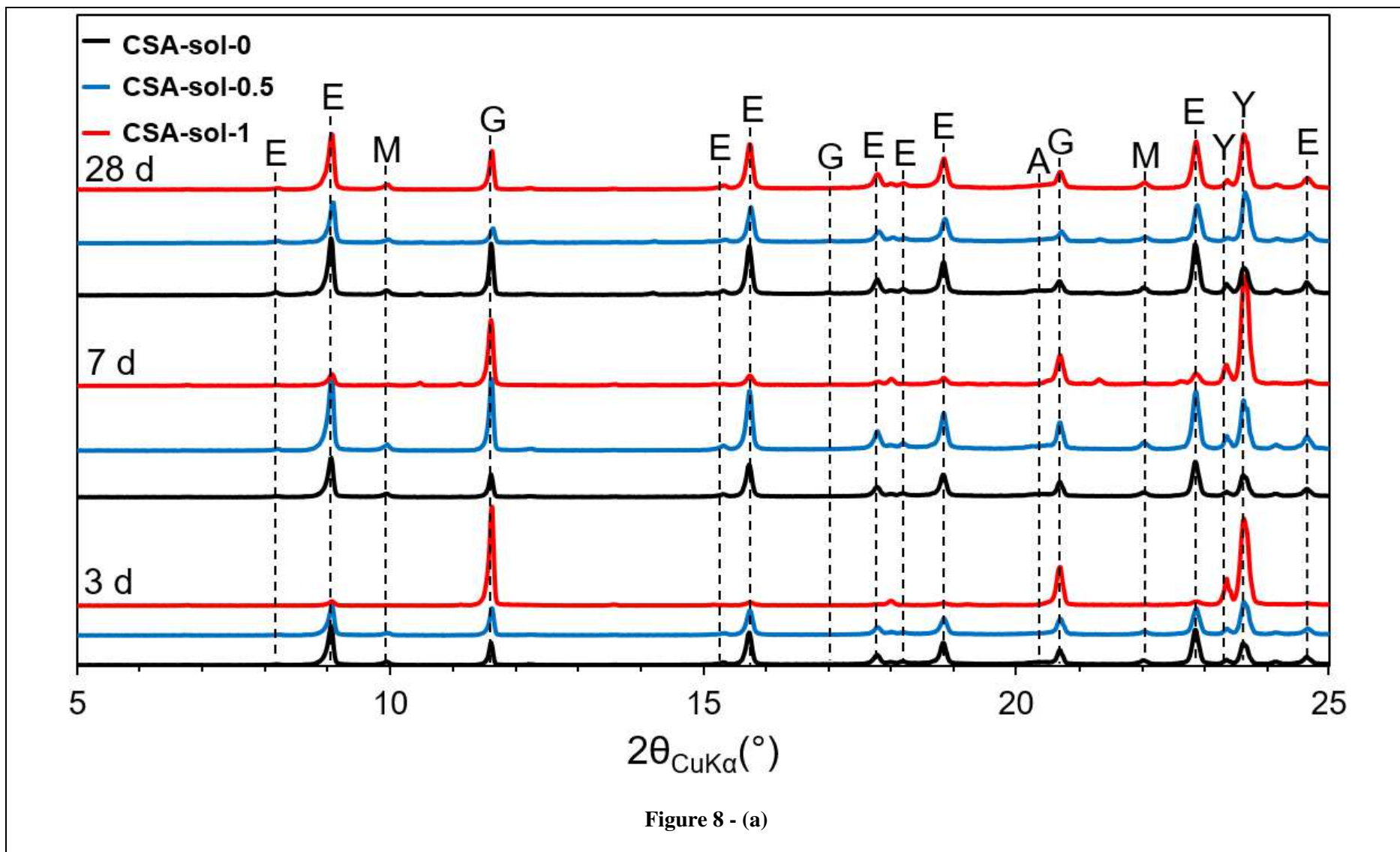


Figure 7 - (a)







**Figure 8 - (a)**

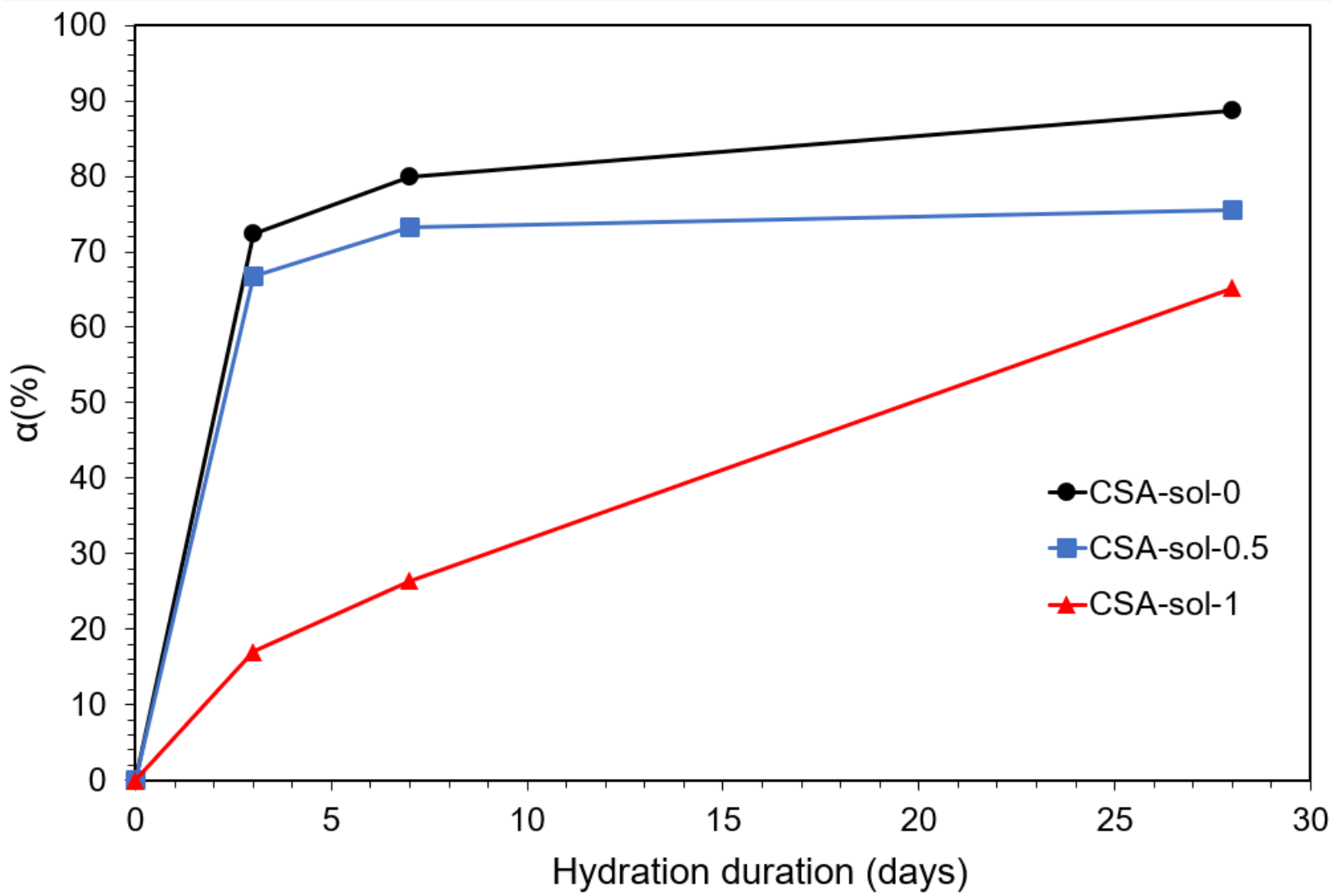
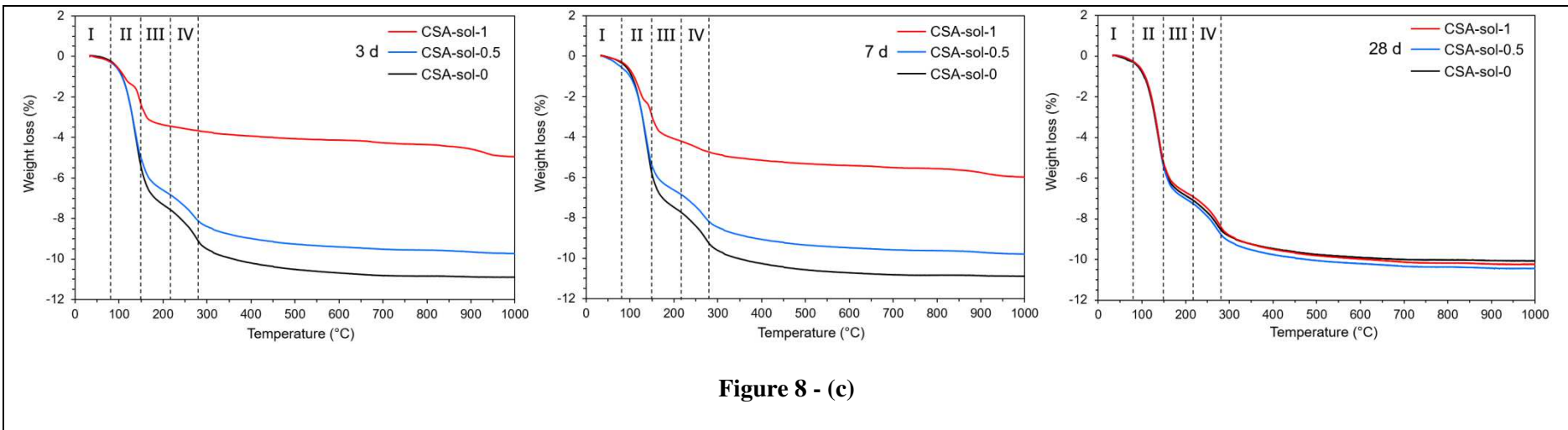


Figure 8 - (b)



### Table captions

Table 1	Presentation of all prepared samples the corresponding performed characterizations techniques.
Table 2	ICSD collection codes used for XRD-Rietveld quantitative analysis.
Table 3	Physical and chemical characteristics of the ye'elimité powders (Ye-sol and Ye-chem).
Table 4	Zeta potential measurements of the prepared ye'elimité suspensions.
Table 5	Results of Rietveld phase analysis (wt.%) for model cements (CSA-sol) and (CSA-Chem) at different hydration ages. Rietveld agreement factors are also given.
Table 6	Results of Rietveld phase analysis (wt.%) for model cements (CSA-sol-0), (CSA-sol-0.5) and (CSA-sol-1) at different hydration ages. Rietveld agreement factors are also given.

**Table 1**

	Sample name	Preparation method	Characterizations
For the study of ye'elimité dissolution (W/C = 1000)	Ye-sol	Fig. 2a	IC / SEM <sup>†</sup>
	Ye-sol-5	Fig. 2b	IC / SEM
	Ye-sol-10	Fig. 2b	IC / SEM
	Ye-chem	Fig. 2a	IC / SEM
For the hydration study of CSA ye'elimité-rich cement (W/C = 2), C = Ye + Gy	CSA-sol-0	Fig. 3-a	XRD-Rietveld analysis TGA-DTG
	CSA-sol-0.5	Fig. 3-b	XRD-Rietveld analysis TGA -DTG
	CSA-sol-1	Fig. 3-b	XRD-Rietveld analysis TGA -DTG
	CSA-chem	Fig. 3-a	XRD-Rietveld analysis TGA -DTG

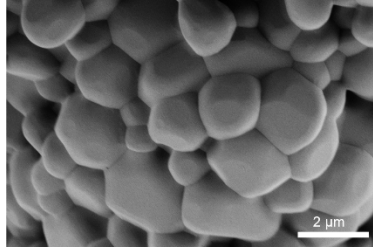
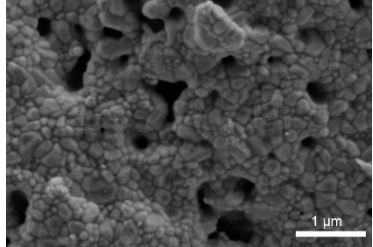
<sup>†</sup> IC: continuous ionic conductivity measurement, SEM: scanning electron microscopy, XRD: X-ray

diffraction, TGA: thermogravimetric analysis, DTG: Derivative thermogravimetry.

**Table 2**

Phase name	Formula	ICSD codes	Ref.
Orthorhombic ye'elimit	$C_4A_3\bar{S}$	237892	[31]
Ettringite	$C_6A\bar{S}_3H_{32}$	155395	[32]
Monosulfoaluminate	$C_4A\bar{S}H_{12}$	100138	[33]
Gibbsite	$AH_3$	6162	[34]
Gypsum	$C\bar{S}H_2$	151692	[35]

**Table 3**

	<b>Ye-sol powder</b>	<b>Ye-chem powder</b>
Synthesis method	Solid-state reactions	Sol-gel chemical route
Synthesis protocol details	Ref. [25]	Ref. [39]
Synthesis temperature (°C)	1300	1250
PSD	d10 ( $\mu\text{m}$ )	3.1
	d50 ( $\mu\text{m}$ )	14.6
	d90 ( $\mu\text{m}$ )	51.1
SSA <sub>BET</sub> ( $\text{m}^2/\text{g}$ )	0.74	2.2
Rietveld analysis	C <sub>4</sub> A <sub>3</sub> S (wt.%)	99.2
	CA (wt.%)	-
	CA <sub>2</sub> (wt.%)	0.8
Microstructure (SEM)		
Ye'elimitate average grain size	$2 \pm 1.2 (\mu\text{m})$	$136 \pm 48 (\text{nm})$

**Table 4**

Ye'elimit suspension	$\zeta$ (mV)
Ye-sol-0	$7.7 \pm 0.3$
Ye-sol-5	$-0.2 \pm 0.1$
Ye-sol-10	$-10.9 \pm 2.8$

**Table 5**

Phase	CSA-sol				CSA-chem			
	t <sub>0</sub>	3 d	7 d	28 d	t <sub>0</sub>	3 d	7 d	28 d
Ye'elimité	63.9	17.6	12.8	7.2	63.9	2.4	1.5	0.7
C <sub>4</sub> A <sub>3</sub> S								
Gypsum	36.1	9.6	8.6	4.5	36.1	1.9	0.8	0.7
C <sub>2</sub> S <sub>2</sub> H <sub>2</sub>								
Ettringite	-	58	65.9	45.0	-	74.1	52.2	83.0
C <sub>6</sub> A <sub>3</sub> S <sub>3</sub> H <sub>32</sub>								
Monosulfo -aluminate	-	0.1	0.1	28.5	-	0.2	29.5	0.5
C <sub>4</sub> A <sub>3</sub> S <sub>12</sub> H <sub>12</sub>								
Gibbsite	-	14.7	12.6	14.8	-	21.4	16.0	15.1
AH <sub>3</sub>								
Sum of hydrate amounts	-	72.8	78.6	88.3	-	95.7	97.7	98.6
R <sub>wp</sub> (%)	-	19.9	18.5	16.8	-	23.1	18.8	21.8
R <sub>exp</sub> (%)	-	2.8	3.6	2.9	-	2.6	2.7	2.6
GOF	-	7.1	5.1	5.8	-	8.7	6.9	8.3

**Table 6**

Phase	CSA-sol-0				CSA-sol-0.5				CSA-sol-1			
	t <sub>0</sub>	3 d	7 d	28 d	t <sub>0</sub>	3 d	7 d	28 d	t <sub>0</sub>	3 d	7 d	28 d
Ye'elimitite C <sub>4</sub> A <sub>3</sub> S	63.9	17.6	12.8	7.2	63.9	21.3	17.1	15.6	63.9	53.0	47.0	22.2
Gypsum CSH <sub>2</sub>	36.1	9.6	8.6	4.5	36.1	13.0	13.1	3.3	36.1	30.5	20.1	10.2
Ettringite C <sub>6</sub> AS <sub>3</sub> H <sub>32</sub>	-	58	65.9	45.0	-	54.2	60.2	39.9	-	8.4	17.1	54.4
Monosulfo -aluminate C <sub>4</sub> ASH <sub>12</sub>	-	0.1	0.1	28.5	-	0.1	0.1	24.0	-	0.1	9.5	0.2
Gibbsite AH <sub>3</sub>	-	14.7	12.6	14.8	-	11.4	9.5	17.2	-	8.0	6.3	13
Sum of hydrate amounts	-	72.8	78.6	88.3	-	65.7	69.8	81.1	-	16.5	32.9	67.6
R <sub>wp</sub> (%)	-	19.9	18.5	16.8	-	18.1	21.4	15.9	-	21.2	17.2	20.4
R <sub>exp</sub> (%)	-	2.8	3.6	2.9	-	3.7	2.7	3.0	-	4.0	3.2	2.8
GOF	-	7.1	5.1	5.8	-	4.9	7.8	5.3	-	5.4	5.4	7.2